JAERI-Research
97-080

A SIMPLE AND RATIONAL NUMERICAL METHOD OF TWO-PHASE FLOW WITH VOLUME-JUNCTION MODEL,(II)
— THE NUMERICAL METHOD FOR GENERAL CONDITION OF TWO-PHASE FLOW IN NON-EQUILIBRIUM STATES —

November 1997

Motoaki OKAZAKI

日本原子力研究所
Japan Atomic Energy Research Institute

本レポートは，日本原子力研究所が不定期に公刊している研究報告書です。
入手の問合わせは，日本原子力研究所研究情報部研究情報課（〒319-11 茨城県那珂郡東海村）あて，お申し越しください。なお，このほかに財団法人原子力弘済会資料センター（〒319-11 茨城県那珂郡東海村日本原子力研究所内）で複写による実費頒布をおこなっております。

This report is issued irregularly.
Inquiries about availability of the reports should be addressed to Research Information Division, Department of Intellectual Resources, Japan Atomic Energy Research Institute, Tokai-mura, Naka-gun, Ibaraki-ken 319-11, Japan.

編集兼発行　日本原子力研究所
印　　刷　㈱原子力資料サービス

JAERI－Research 97－080

A Simple and Rational Numerical Method of Two-phase Flow with Volume-Junction Model,(Ⅱ) —The Numerical Method for General Condition of Two-phase Flow in Non-equilibrium States—

Motoaki OKAZAKI

Department of Reactor Engineering
Tokai Research Establishment
Japan Atomic Energy Research Institute
Tokai-mura, Naka-gun, Ibaraki-ken

(Received October 2, 1997)

In the previous report[1], the usefulness of a new numerical method to achieve a rigorous numerical calculation using a simple explicit method with the volume-junction model was presented with the verification calculation for the depressurization of a saturated two-phase mixture. In this report, on the basis of solution method above, a numerical method for general condition of two-phase flow in non-equilibrium states is presented. In general condition of two-phase flow, the combinations of saturated and non-saturated conditions of each phase are considered in the each flow of volume and junction. Numerical evaluation programs are separately prepared for each combination of flow condition. Several numerical calculations of various kinds of non-equilibrium two-phase flow are made to examine the validity of the numerical method. Calculated results showed that the thermodynamic states obtained in different solution schemes were consistent with each other. In the first scheme, the states are determined by using the steam table as a function of pressure and specific enthalpy which are obtained as the solutions of simultaneous equations. In the second scheme, density and specific enthalpy of each phase are directly calculated by using conservation equations of mass and enthalpy of each phase, respectively. Further, no accumulation of error in mass and energy was found. As for the specific enthalpy, two cases of using energy equations for the volume are examined. The first case uses total energy conservation equation and the second case uses the type of the first law of thermodynamics. The results of both cases agreed well.

Keywords: Two-phase Flow Analysis Code, Non-equilibrium State, Numerical Method

Volume-Junction法による二相流の単純で合理的な数値解法（Ⅱ）
― 熱力学的非平衡を含む二相流の一般条件に対する数値解法 ―

日本原子力研究所東海研究所原子炉工学部
岡崎　元昭

（1997年10月2日受理）

前報に於て、Volume-Junctionモデルを用いた場合の、陽解法による単純で合理的な数値解法を新しく提出し、その有用性を減圧過程の飽和二相流の解析によって示した。

本報では、同じ解法に基づいた、熱力学的非平衡を含む一般の二相流に対する数値解法について述べる。一般条件の二相流においてはVolume内及びJunction内に夫々、気液各相の飽和、非飽和の組み合わせがある。それらを分類して個別に流れの変化を評価している。

本数値解法を検証するため種々の非平衡二相流に対していくつかの数値解析を行った。その結果、以下のことを確認した。連立方程式の解として得られた圧力と比エンタルピから蒸気表を用いて得られる状態量と、質量保存式及びエネルギ式から気液各相について得られる密度変化、比エンタルピ変化との整合性。質量及びエネルギに対する誤差の蓄積のないこと。さらに、比エンタルピについてはVolume内エネルギ式として全エネルギ保存式を用いる場合と熱力学第一法則の形の式を用いる場合を比較し、両者が一致すること。

東海研究所：〒319-11　茨城県那珂郡東海村白方白根2-4

Contents

目　　次

1. Introduction

In the previous report[1], the author showed the validity of basic equation based on the rigorously derived phase change equation of each phase in saturated condition and the validity of the simple explicit numerical method with the volume-junction model by making some numerical calculation for each phase independently to show the consistency between solutions for two different solution schemes and to show no accumulation of error in mass and energy. To achieve the rigorous numerical calculation, difference equations for numerical model were carefully derived so as to preserve the physical meaning of the basic equations.

Specifically, momentum equations for the flow in the volume are newly derived to keep the strict conservation of energy in the volume.

Basic equations of the partial differential form in this report for unsteady two-phase flow are quoted from the paper[2] the same as used in the previous report[1].

We present the integrated analyzing method of general condition of two-phase flow of equilibrium through non-equilibrium state as described in the chapter 2.

The numbers of unknowns and equations for a special where both phases are non-equilibrium state are as follows.

In the partial differential equations :

Unknowns : $u_g, u_\ell, P, \alpha, T_g, T_\ell, w_{\ell g}$ Total 7

Equations :2-Mass conservation, 2-Momentum balance,
2-Total energy conservation equation,
Condensation equation due to temperature difference Total 7

In the volume-junction model :

Unknowns : - for junction flow : $w_{g,J}, w_{\ell,J}, \Delta h_{g,J}, \Delta h_{\ell,J}$

- for the fluid in volume : $P, \alpha, T_g, T_\ell, W_{g,Vol}, W_{\ell,Vol}, \dot{M}_{ZC}$ Total 11

Equations : - for junction flow : 2-Momentum balance,
2-First law of thermodynamics.
- for the fluid in volume : 2-Mass conservation,
2-Total energy conservation, 2-First law of thermodynamics,
Condensation equation due to temperature difference
Total 11

The basic equations for the numerical use with the volume-junction model are derived in the same manner as described in Reference[1].

The outline , how the unknowns are solved in the analysis of non-equilibrium two-phase flow, is explained as follows.

The actual procedure of numerical calculation is described in the section 4.4.

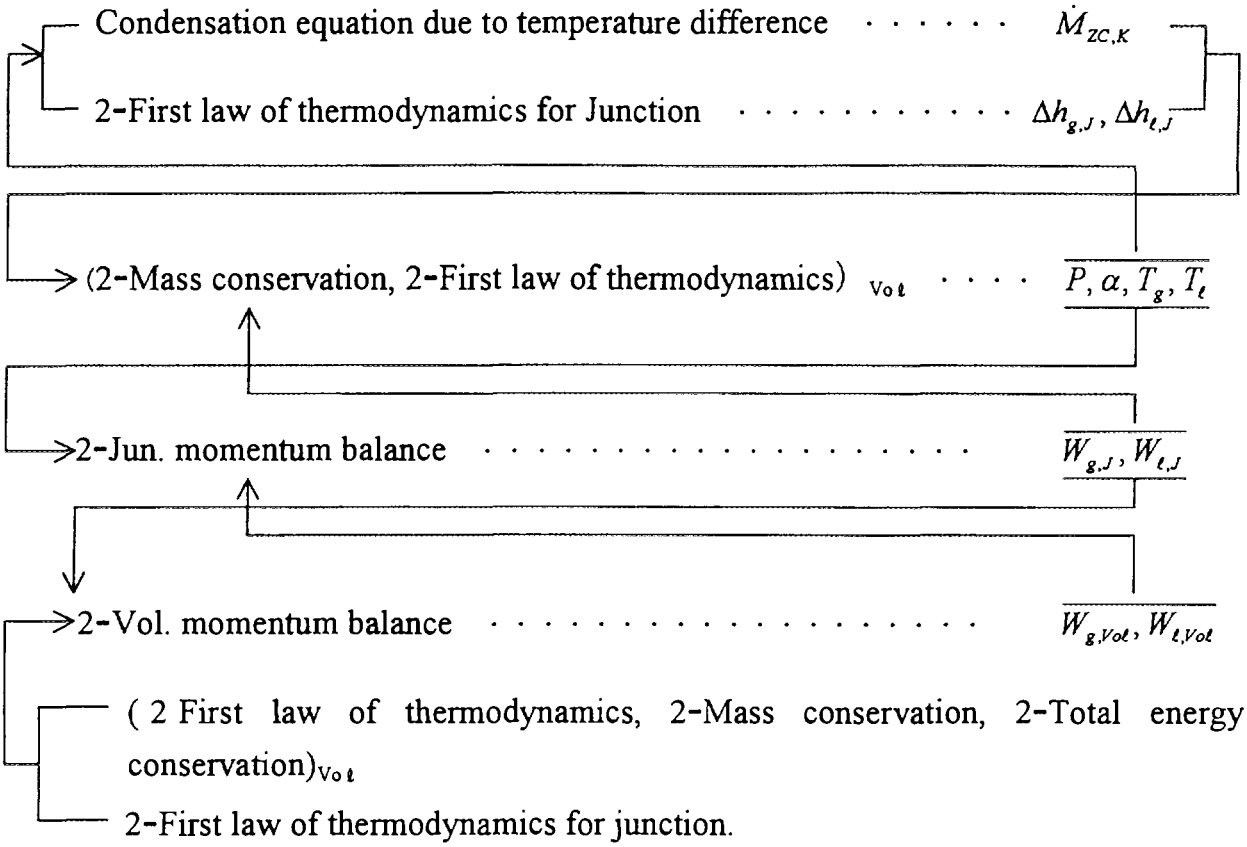

Condensation rate between vapor and liquid due to temperature difference in a volume $\dot{M}_{ZC,K}$ is evaluated by using the empirical correlation with the condensation heat transfer coefficient. The inlet enthalpy to a downstream volume is determined by evaluating the enthalpy change of each phase in a junction flow $\Delta h_{g,J}, \Delta h_{\ell,J}$. Thermodynamic states in a volume P, α, T_g, T_ℓ are obtained by solving the mass conservation equation and the equation of the first law of thermodynamics of each phase simultaneously. The junction flow rate is determined by the momentum balance equation for the junction flow with the momentum change from volume to junction and with the pressure difference between volumes. Volume flow rate is determined by

the momentum balance equation in the volume which is derived by combining the first law of thermodynamics, mass conservation and total energy conservation of each phase in the volume, and the first law of thermodynamics of each phase in the junction flow.

Some numerical calculations for the non-equilibrium two-phase flow specified by cases in the chapter 2 are made for the purpose to verify that the proposed numerical method works correctly by presenting the consistency between solutions and no accumulation of error in mass and energy in the calculation proceeding.

The thermodynamic state of each phase in the volume is obtained in two different solution schemes as follows.

At first, we have already obtained the state values of P, α, T_g, T_ℓ using the equations of mass conservation and the first law of thermodynamics simultaneously as mentioned above. Then, using only the mass conservation equation of gas or liquid phase and void fraction α, the density of gas ρ_g or liquid ρ_ℓ is determined. Further, using only the equation of the first law of thermodynamics of gas or liquid phase and pressure increment ΔP, the specific enthalpy of gas h_g or liquid h_ℓ is determined.

On the other hand, from the steam table as a function of P and h_g or h_ℓ, density ρ_{gST} and temperature T_{gPU} of gas or $\rho_{\ell ST}$ and $T_{\ell PU}$ of liquid are obtained. Saturated temperature T_s of pressure P is also obtained. Thus, we can compare ρ_g, ρ_ℓ with ρ_{gST}, $\rho_{\ell ST}$ and T_g, T_ℓ with T_{gPU}, $T_{\ell PU}$.

Moreover, after substituting the mass increment obtained from the mass conservation equation and kinetic energy increment from momentum balance equation for the volume flow of gas phase into the total energy conservation equation of gas phase, the specific internal energy change of the gas phase is calculated. The specific internal energy of gas e_{gE} is therefore calculated by integration and converted to specific enthalpy using the relation $h_{gST}=e_{gE}+P/\rho_g$. The specific enthalpy of liquid $h_{\ell ST}$ is also calculated in the same way as the gas phase. Thus, we can compare h_g, h_ℓ obtained from the relational expression of thermodynamical state change, with h_{gST}, $h_{\ell ST}$ obtained from total energy conservation equation. The numerical calculation is advanced using ρ_g, ρ_ℓ obtained from mass conservation equation and h_g,h_ℓ from the relational expression of thermodynamical state change, for the initial values of a next

step with the simple explicit solution method.

Accordingly, if the thermodynamic states obtained in two different schemes mentioned above coincide with each other and if the summation of the total energy dealt with in a whole calculation model is conserved at any time during the calculation, the correctness of calculation with the proposed numerical method will be proved.

2 Classification of state conditions for numerical solution scheme.

Non-equilibrium conditions dealt with in this report are superheated for gas phase and subcooled for liquid phase. These non-equilibrium states appear in increasing pressure. However, superheated water and subcooled vapor which appear in a very rapid decreasing pressure as the result of evaporation lag in the liquid and condensation lag in the gas, respectively, are not dealt with in this report. Possible combinations of the thermodynamic state of each phase in a volume are as presented in the Table.1.

Table.1 Combinations of state of gas and liquid in a volume.

Type	Gas	Liquid
A	Saturated	Saturated
B	Saturated	subcooled
C	Superheated	saturated
D	Superheated	subcooled

Possible combinations of thermodynamic state changes of each phase in the flow from volume to volume are classified as in the Table.2 where no external heat is considered. External heat is considered in a volume as described in chapter 4.

Table.2 Classifications of state changes in the flow from volume to volume.

Type	Gas	Liquid	ΔP along flow path
a	all satu.	all satu.	$\Delta P<0$
b	all satu.	subc.-satu.	$\Delta P<0$
c	all satu.	all subc.	$\Delta P<0$
d	all super.	all satu.	$\Delta P<0$
e	all super.	subc.-satu.	$\Delta P<0$
f	super.-satu.	all satu.	$\Delta P<0$
g	super.-satu.	subc.-satu.	$\Delta P<0$
h	super.-satu.	all subc.	$\Delta P<0$
i	all super.	all subc.	$\Delta P>0$ or <0

Note : satu : saturated
super : superheated
subc : subcooled

These state changes mostly occur in cases where pressure decreases except in the case "i". Combining the Table.1 and Table.2, we can show the variations of state changes in the flow from volume to volume inlet in Fig.1.

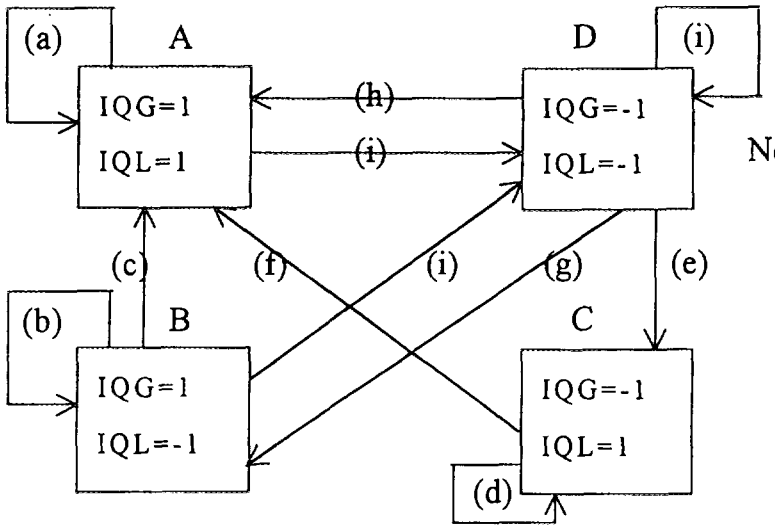

Note : IQG and IQL are flags for state of gas and liquid.
1 : saturated
-1 : non-equilibrium

Fig.1 Diagram of states changes from Volume to Volume inlet.

This diagram shows the possible changes in the flow from each of state A,B,C,D in volume to the downstream volume inlet. So, lines C→D and A→B are omitted since they are possible only when negative external heat is added to the liquid. Line A→C is also omitted which is possible only when negative external heat is added to the vapor. All cases of state changes shown in Fig.1 are arranged in the coding program considering flow direction and the pressure change.

State flag of each phase IQG, IQL is determined for the new time step after pressure change ΔP in a volume is estimated, as follows.

・IQG=1(saturated vapor)

1 For old IQG=1, if $\Delta P<0$ and $\dot{M}_{tC}>0$ occur.

2 For old IQG=－1, if $h_g \leqq h_{gs}$ occurs for any of $\Delta P>0, \Delta P<0$.

・IQL=1(saturated water)

1 For old IQL=1, if $\dot{M}_{tE}>0$ occur for any of $\Delta P>0, \Delta P<0$.

2 For old IQL=－1, if $h_l \geqq h_{ls}$ occurs for any of $\Delta P>0, \Delta P<0$.

・IQG=－1(superheated vapor)

1 If $\Delta P>0$ occurs for any of old IQG.

2 If $\Delta P<0$ and $\dot{M}_{tC}<0$ occur for any of old IQG.

3 For old IQG=－1, if $h_g \geqq h_{gs}$ occurs for any of $\Delta P>0, \Delta P<0$.

・IQL=－1(subcooled water)

1 If $\Delta P>0$ and $\dot{M}_{tE}<0$ occur for any of old IQL.

2 For old IQL=1, if $\Delta P<0$ and $\dot{M}_{tE}<0$ occurs.

3 For old IQL=－1, if $h_l \geqq h_{ls}$ occur for any of $\Delta P>0$, $\Delta P<0$.

3. Equations for numerical solution with the volume-junction model.

The general basic equations of unsteady two-phase flow with non-equilibrium states for volume-junction model are expressed as follows by reference to the previous paper[2]. Energy equations are expressed so as to preserve the physical meaning of differential equations. The difference equations for the actual numerical use are reduced to simpler forms so that calculation can be made more precise as described in the chapter 4.

We consider the conservation law for the volume "K" in a volume-junction model of constant area flow as shown in Fig.2.

3.1 Basic equations

Mass conservation:

$$\frac{\Delta M_{g,K}}{\Delta t} = W_{g,J-1} - W_{g,J} + \left(\dot{M}_{tE} - \dot{M}_{tC} - \dot{M}_{ZC}\right)_K + \left(\dot{M}_{ZE} - \dot{M}_{ZC}\right)_{J-1} \tag{1}$$

$$\frac{\Delta M_{l,k}}{\Delta t} = W_{l,J-1} - W_{l,J} + \left(\dot{M}_{tE} - \dot{M}_{tC} - \dot{M}_{ZC}\right)_K - \left(\dot{M}_{ZE} - \dot{M}_{ZC}\right)_{J-1} \tag{2}$$

Energy conservation :

$$\begin{aligned}
&\frac{\Delta}{\Delta t}\left\{M_g\left(e_g + \frac{u_g^2}{2} + gz\cos\theta\right)\right\}_K = W_{g,J-1}\left(h_g + \frac{u_g^2}{2} + gz\cos\theta\right)_I \\
&-\left(W_{g,J} + \dot{M}_{ZC,K}\right)\left(h_g + \frac{u_g^2}{2} + gz\cos\theta\right)_K + \dot{M}_{tE,K}\left(h_{gs} + \frac{u_l^2}{2} + gz\cos\theta\right)_K \\
&-\dot{M}_{tC,K}\left(h_{ls} + \frac{u_g^2}{2} + gz\cos\theta\right)_K + \int_I^K h_{gs}\cdot\Delta\dot{M}_{ZE} + M_{ZE,J-1}\left(\frac{u_l^2}{2} + gz\cos\theta\right)_I \\
&-\int_I^K h_{ls}\cdot\Delta\dot{M}_{ZC} - \dot{M}_{ZC,J-1}\left(\frac{u_g^2}{2} + gz\cos\theta\right)_I - PV\frac{\Delta\alpha}{\Delta t} + \left(W_g\cdot\Delta\dot{q}_{Eg}\right)_{J-1} + \left(M_g\frac{\Delta q_{Eg}^0}{\Delta t}\right)_K
\end{aligned} \tag{3}$$

$$\frac{\Delta}{\Delta t}\left\{M_l\left(e_l+\frac{u_l^2}{2}+gz\cos\theta\right)\right\}_K = W_{l,J-1}\left(h_l+\frac{u_l^2}{2}+gz\cos\theta\right)_l$$
$$-W_{l,J}\left(h_l+\frac{u_l^2}{2}+gz\cos\theta\right)_K+\dot{M}_{ZC,K}\left(h_g+\frac{u_g^2}{2}+gz\cos\theta\right)_K$$
$$-\dot{M}_{lE,K}\left(h_{gs}+\frac{u_l^2}{2}+gz\cos\theta\right)_K+\dot{M}_{lC,K}\left(h_{ls}+\frac{u_g^2}{2}+gz\cos\theta\right)_K-\int_l^K h_{gs}\cdot\Delta\dot{M}_{ZE}$$
$$-\dot{M}_{ZE,J-1}\left(\frac{u_l^2}{2}+gz\cos\theta\right)_l+\int_l^K h_{ls}\cdot\Delta\dot{M}_{ZC}+\dot{M}_{ZC,J-1}\left(\frac{u_g^2}{2}+gz\cos\theta\right)_l$$
$$+PV\frac{\Delta\alpha}{\Delta t}+\left(W_l\cdot\Delta\dot{q}_{El}\right)_{J-1}+\left(M_l\frac{\Delta q_{El}^0}{\Delta t}\right)_K \qquad (4)$$

We consider the momentum balance for the junction "J", in Fig.2.

Momentum balance :

$$\Delta Z_K\frac{\Delta W_{g,J}}{\Delta t}=\left(W_g\cdot u_g\right)_K-\left(W_g\cdot u_g\right)_J-\dot{M}_{ZE,J}\cdot\left(u_g-u_l\right)_J-\dot{M}_{lE,K}\cdot\left(u_g-u_l\right)_K-M_{g,K}\cdot g\cos\theta$$
$$-\left(\Delta F_{wg}+\Delta F_{gl}\right)_J+A_{g,J}\cdot\left(P_K-P_L\right) \qquad (5)$$

$$\Delta Z_K\cdot\frac{\Delta W_{l,J}}{\Delta t}=\left(W_l\cdot u_l\right)_K-\left(W_l\cdot u_l\right)_J+\dot{M}_{ZC,J}\cdot\left(u_g-u_l\right)_J+\left(\dot{M}_{lC}+\dot{M}_{ZC}\right)_K\cdot\left(u_g-u_l\right)_K$$
$$-M_{l,K}\cdot g\cos\theta-\left(\Delta F_{wl}+\Delta F_{lg}\right)_J+A_{l,J}\cdot\left(P_K-P_L\right) \qquad (6)$$

3.2 State change equations

Basically, the energy change in the volume can be obtained by using the energy conservation equations. However, for the evaluation of enthalpy change in a flow it is easier and will give the more precise calculation to use the equations of the first law of thermodynamics concerning the state change in the flow than using the total energy conservation equations. The state change in the flow of junction and of volume must necessarily be considered separately. Therefore, we can classify the heat contributing to the state change in the flow of the volume-junction model as follows.

3.2.1 Heat contributing to the state change of the two-phase flow.

We can define the heat to be distributed to the fluids in a volume and the fluids in a junction flow, as follows.

(1) Heat distributed to the flow from Vol.I to Vol.K.

- Frictional heat arisen at wall and interphase.
- Latent heat transfer caused by phase change and mixing frictional heat due to

moving into another phase in the junction flow.

· Mixing frictional heat due to mixing of fluids from the upstream volume.

(2) Heat distributed to the fluids in Vol.K.

· Heat transported by the fluids from Vol.I whose state is evaluated at the pressure in Vol.K considering the state change in the flow of junction J-1.

· Latent heat transfer caused by phase change and mixing frictional heat due to moving into another phase in the volume.

· External heat.

3.2.2 State change in junction flow.

The state change in the flow from Vol.I to Vol.K is first evaluated for a small pressure difference of the flow by dividing ($P_I - P_K$) into n equal parts. In a small difference pressure of I-th ΔP, enthalpy change of each phase is expressed by the first law of thermodynamics as follows by reference to Eqs.(8A) and (8B) in the previous report[1].

$$\Delta h_{g,J-1}^{(i)} = \left(\Delta q_{TPg} + \frac{\Delta P}{\rho_g} + r \frac{\Delta \dot{M}_{ZC}}{W_g} \right)_{J-1}^{(i)} \tag{7}$$

$$\Delta h_{l,J-1}^{(i)} = \left(\Delta q_{TPl} + \frac{\Delta P}{\rho_l} - r \frac{\Delta \dot{M}_{ZE}}{W_l} \right)_{J-1}^{(i)} \tag{8}$$

Where, the heat added to the junction flow of each phase is defined in the section 1-(1), as follows.

$$\begin{aligned} \left(W_l \cdot \Delta q_{TPl}\right)_{J-1}^{(i)} = & \left\{ u_l \left(\Delta F_{Wl} + \Delta F_{lg} \right) + \Delta \dot{Q}_{El} + W_l \cdot \Delta q_{ml} \right\}_{J-1} \cdot \frac{1}{n} \\ & - \left(\Delta q_{ml} \cdot \Delta \dot{M}_{ZE} - C_1 \cdot \Delta \dot{M}_{ZC} \right)_{J-1}^{(i)} \end{aligned} \tag{9}$$

$$\begin{aligned} \left(W_g \cdot \Delta q_{TPg}\right)_{J-1}^{(i)} = & \left\{ u_g \left(\Delta F_{Wg} + \Delta F_{gl} \right) + \Delta \dot{Q}_{Eg} + W_g \cdot \Delta q_{mg} \right\}_{J-1} \cdot \frac{1}{n} \\ & - \left(\Delta q_{mg} \cdot \Delta \dot{M}_{ZC} - C_2 \cdot \Delta \dot{M}_{ZE} \right)_{J-1}^{(i)} \end{aligned} \tag{10}$$

These are the same as Eqs (17) and (18) of previous report[1]. So, the phase change rates $\dot{M}_{ZE,J-1}$ and $\dot{M}_{ZC,J-1}$ are evaluated in the same way.

Where

$$\left.\begin{aligned} C_1 &= \frac{1}{2}\left(u_{g,J} - u_{l,K}\right)^2, \qquad C_2 = \frac{1}{2}\left(u_{l,J} - u_{g,K}\right)^2 \\ \Delta q_{ml} &= \frac{1}{2}\left(u_{l,K} - u_{l,J}\right)^2, \qquad \Delta q_{mg} = \frac{1}{2}\left(u_{g,K} - u_{g,J}\right)^2 \end{aligned}\right\} \tag{11}$$

The enthalpy of each phase at the inlet of vol.K, $h_{g,Ki}$ and $h_{l,Ki}$ can be obtained from Eqs.(7) and (8), respectively, by integrating with pressure from P_I to P_K.

3.2.3 State change in the volume

Enthalpy change of each phase in the volume can be expressed by using the first law of thermodynamics with consideration of heat added to each phase as defined in the section 2.1-(2) of this chapter.

$$\Delta h_{g,K} = \left(\Delta q_{TPg} + \frac{\Delta P}{\rho_g} + r \cdot \frac{\dot{M}_{tC}}{M_g} \cdot \Delta t\right)_K \tag{12}$$

$$\Delta h_{l,K} = \left(\Delta q_{TPl} + \frac{\Delta P}{\rho_l} - r \cdot \frac{\dot{M}_{tE}}{M_l} \cdot \Delta t\right)_K \tag{13}$$

Where

$$\begin{aligned} \left(M_g \cdot \Delta q_{TPg}\right)_K = {} & \left(W_g - \dot{M}_{ZC}\right)_{J-1} \cdot \left(h_{g,Ki} - h_{g,K}\right) + \dot{M}_{ZE,J-1}\left(h_{gs} - h_g\right)_K + \frac{\Delta Q^0_{Eg}}{\Delta t} \\ & + \dot{M}_{tE,K}\left\{\left(h_{gs} - h_g\right) + \frac{1}{2}\left(u_g - u_l\right)^2\right\}_K \end{aligned} \tag{14}$$

$$\begin{aligned} \left(M_l \cdot \Delta q_{TPl}\right)_K = {} & \left(W_l - \dot{M}_{ZE}\right)_{J-1} \cdot \left(h_{l,Ki} - h_{l,K}\right) + \dot{M}_{ZC,J-1}\left(h_{ls} - h_l\right)_K + \frac{\Delta Q^0_{El}}{\Delta t} \\ & + \dot{M}_{tC,K}\left\{\left(h_{ls} - h_l\right) + \frac{1}{2}\left(u_g - u_l\right)^2\right\}_K + \dot{M}_{ZC,K}\left\{\left(h_g - h_l\right) + \frac{1}{2}\left(u_g - u_l\right)^2\right\}_K \end{aligned} \tag{15}$$

The equation of phase change rate in each phase can be derived in the same way as presented in the previous report[1].

$$\dot{M}_{tE} = \frac{1}{y_6}\left(y_7 \frac{\Delta P}{\Delta t} + y_8\right) \tag{16}$$

$$\dot{M}_{tC} = -\frac{1}{y_6}\left(y_9 \frac{\Delta P}{\Delta t} + y_{10}\right) \tag{17}$$

Where,

$$
\left.
\begin{aligned}
y_6 &= \begin{cases} 1+C_6^2 & (for\ IQG = IQL = 1) \\ 1 & (for\ IQG = -1\ \ or\ \ IQL = -1) \end{cases} \\
C_6 &= C_5 / r,\ \ C_5 = \left(u_g - u_l\right)_K^2 / 2 \\
y_7 &= \begin{cases} EP + CP \cdot C_6 & (for\ IQG = IQL = 1) \\ EP \ \ (for\ IQL = 1), & 0.0\ (for\ IQG = 1) \end{cases} \\
y_9 &= \begin{cases} EP \cdot C_6 - CP & (for\ IQG = IQL = 1) \\ 0.0 \ \ (for\ IQL = 1), & -CP\ (for\ IQG = 1) \end{cases} \\
EP &= -\frac{M_l}{r}\left\{\left(\frac{dh_l}{dP}\right)_{sat} - \frac{1}{\rho_l}\right\} \\
CP &= -\frac{M_g}{r}\left\{\left(\frac{dh_g}{dP}\right)_{sat} - \frac{1}{\rho_g}\right\} \\
y_8 &= \begin{cases} \left\{\dfrac{\Delta Q_{El}^0}{\Delta t} + C_{11} - C_6\left(\dfrac{\Delta Q_{Eg}^0}{\Delta t} + C_{10}\right)\right\}\dfrac{1}{r}, & (for\ IQG = 1,) \\ \left\{\dfrac{\Delta Q_{El}^0}{\Delta t} + C_{11} + \dot{M}_{ZC,K}\left(C_5 + h_g - h_{ls}\right)\right\}\dfrac{1}{r}, & (for\ IQG = -1) \\ 0.0 & (for\ IQL = -1,\ for\ any\ IQG) \end{cases} \\
y_9 &= \begin{cases} \left\{C_6\left(\dfrac{\Delta Q_{El}^0}{\Delta t} + C_{11}\right) + \dfrac{\Delta Q_{Eg}^0}{\Delta t} + C_{10}\right\}\dfrac{1}{r}, & (for\ IQL = 1,) \\ \left(\dfrac{\Delta Q_{Eg}^0}{\Delta t} + C_{10}\right)\dfrac{1}{r}, & (for\ IQL = -1) \\ 0.0 & (for\ IQG = -1,\ for\ any\ IQL) \end{cases} \\
C_{10} &= \left(W_g - \dot{M}_{ZC}\right)_{J-1} \cdot \left(h_{g,Ki} - h_{g,K}\right) + \dot{M}_{ZE,J-1}\left(h_{gs} - h_g\right)_K \\
C_{11} &= \left(W_l - \dot{M}_{ZE}\right)_{J-1} \cdot \left(h_{l,Ki} - h_{l,K}\right) + \dot{M}_{ZC,J-1}\left(h_{ls} - h_l\right)_K
\end{aligned}
\right\} \qquad (18)
$$

3.3 Derivation of momentum equations for the flow in the volume.

Momentum equations in the volume are derived to keep strict energy conservation in the volume and are essentially the same as derived from saturated two-phase flow in the previous report. For the general conditions of two-phase flow with non-equilibrium states, momentum equations in the volume are expressed as follows.

$$\left(\Delta Z\cdot\frac{\Delta W_g}{\Delta t}\right)_K=\left\{\frac{1}{2}\frac{(1-B_1)}{u_{g,K}}\left(u_{g,J}-u_{g,K}\right)^2+u_{g,J}\right\}\cdot W_{g,J-1}-W_{g,J}\cdot u_{g,K}$$
$$+\left(\dot{M}_{tE}\cdot u_l\right)_K-\left(\dot{M}_{tC}+\dot{M}_{ZC}\right)_K\cdot u_{g,K}+\left\{\frac{1}{2}\frac{\left(\dot{M}_{ZE,J-1}-B_2\right)}{u_{g,K}}\left(u_{l,J}-u_{g,K}\right)^2+\dot{M}_{ZE,J-1}\cdot u_{l,J}\right\}$$
$$-\left\{\frac{1}{2}\frac{\left(\dot{M}_{ZC,J-1}-B_3\right)}{u_{g,K}}\left(u_{g,J}-u_{g,K}\right)^2+\dot{M}_{ZC,J-1}\cdot u_{g,J}\right\}$$
$$+\left\{\sum_{i=i_l}^{n}\left(h_{gs}\cdot\Delta\dot{M}_{ZE}\right)_{J-1}^{(i)}-h_{gs,K}\cdot\dot{M}_{ZE,J-1}\right\}\frac{1}{u_{g,K}}$$
$$-\left\{\sum_{i=i_g}^{n}\left(h_{ls}\cdot\Delta\dot{M}_{ZC}\right)_{J-1}^{(i)}-h_{gs,K}\cdot\dot{M}_{ZC,J-1}+W_{g,J-1}\sum_{i=i_g}^{n}\left(\frac{r\cdot\Delta\dot{M}_{ZC}}{W_g}\right)_{J-1}^{(i)}\right\}\frac{1}{u_{g,K}}$$
$$-B_1\left(\Delta F_{Wg}+\Delta F_{gl}\right)_{J-1}\cdot\frac{u_{g,J-1}}{u_{g,K}}+\frac{1-B_1}{u_{g,K}}\cdot\Delta\dot{Q}_{Eg}-\frac{W_{g,J-1}}{u_{g,K}}\sum_{i=1}^{n}\left(\frac{\Delta P}{\rho_g}\right)_{J-1}^{(i)}$$
$$-\left(W_g+\dot{M}_{ZE}-\dot{M}_{ZC}\right)_{J-1}\frac{1}{u_{g,K}}g\cos\theta\cdot\left(Z_K-Z_l\right)\qquad(19)$$

$$\left(\Delta Z\cdot\frac{\Delta W_l}{\Delta t}\right)_K=\left\{\frac{1}{2}\frac{(1-B_4)}{u_{l,K}}\left(u_{l,J}-u_{l,K}\right)^2+u_{l,J}\right\}\cdot W_{l,J-1}-W_{l,J}\cdot u_{l,K}$$
$$-\left(\dot{M}_{tE}\cdot u_l\right)_K+\left(\dot{M}_{tC}+\dot{M}_{ZC}\right)_K\cdot u_{g,K}+\left\{\frac{1}{2}\frac{\left(\dot{M}_{ZC,J-1}-B_5\right)}{u_{l,K}}\left(u_{g,J}-u_{l,K}\right)^2+\dot{M}_{ZC,J-1}\cdot u_{g,J}\right\}$$
$$-\left\{\frac{1}{2}\frac{\left(\dot{M}_{ZE,J-1}-B_6\right)}{u_{l,K}}\left(u_{l,J}-u_{l,K}\right)^2+\dot{M}_{ZE,J-1}\cdot u_{l,J}\right\}$$
$$+\left\{\sum_{i=i_g}^{n}\left(h_{ls}\cdot\Delta\dot{M}_{ZC}\right)_{J-1}^{(i)}-h_{ls,K}\cdot\dot{M}_{ZC,J-1}\right\}\frac{1}{u_{l,K}}$$
$$-\left\{\sum_{i=i_l}^{n}\left(h_{gs}\cdot\Delta\dot{M}_{ZE}\right)_{J-1}^{(i)}-h_{ls,K}\cdot\dot{M}_{ZE,J-1}-W_{l,J-1}\sum_{i=i_l}^{n}\left(\frac{r\cdot\Delta\dot{M}_{ZE}}{W_l}\right)_{J-1}^{(i)}\right\}\frac{1}{u_{l,K}}$$
$$-B_4\left(\Delta F_{Wl}+\Delta F_{lg}\right)_{J-1}\cdot\frac{u_{l,J-1}}{u_{l,K}}+\frac{1-B_4}{u_{l,K}}\cdot\Delta\dot{Q}_{El}-\frac{W_{l,J-1}}{u_{l,K}}\sum_{i=1}^{n}\left(\frac{\Delta P}{\rho_l}\right)_{J-1}^{(i)}$$
$$-\left(W_l-\dot{M}_{ZE}+\dot{M}_{ZC}\right)_{J-1}\frac{1}{u_{l,K}}\cdot g\cos\theta\cdot\left(Z_K-Z_l\right)\qquad(20)$$

Where

$$
\left.
\begin{aligned}
B_1 &= \frac{i_j - 1}{n} + \frac{W_{g,J-1}}{n}\sum_{i=i_j}^{n}\left(\frac{1}{W_g}\right)_{J-1}^{(i)}, \quad & B_4 &= \frac{i_j - 1}{n} + \frac{W_{l,J-1}}{n}\sum_{i=i_j}^{n}\left(\frac{1}{W_l}\right)_{J-1}^{(i)} \\
B_2 &= W_{g,J-1}\sum_{i=i_l}^{n}\left(\frac{\Delta \dot{M}_{ZE}}{W_g}\right)_{J-1}^{(i)}, & B_5 &= W_{l,J-1}\sum_{i=i_g}^{n}\left(\frac{\Delta \dot{M}_{ZC}}{W_l}\right)_{J-1}^{(i)} \\
B_3 &= W_{g,J-1}\sum_{i=i_g}^{n}\left(\frac{\Delta \dot{M}_{ZC}}{W_g}\right)_{J-1}^{(i)}, & B_6 &= W_{l,J-1}\sum_{i=i_l}^{n}\left(\frac{\Delta \dot{M}_{ZE}}{W_l}\right)_{J-1}^{(i)}
\end{aligned}
\right\} \qquad (21)
$$

Note ;

i_g : number of vapor became saturated in junction flow

i_l : number of liquid became saturated in junction flow

i_j : smaller number between i_g and i_l

3.4 Constitutive equations.

The equations of the frictional force of wall and interphase are used by the same ones presented in the previous report[1].

Further, condensation equation of vapor to water, induced by the temperature difference is introduced as follows.

$$Q_{cond} = H \cdot A_{gl} \cdot \left(T_g - T_l\right) \cdot V \qquad (22)$$

Where, interphase area per unit volume A_{gl} is calculated assuming flow pattern is annular and the interphase heat transfer coefficient H is approximately 10 kW/m^{2}K, in this report. Condensation rate in Vol. K is

$$\dot{M}_{TC,K} = \frac{Q_{cond}}{h_g - h_l} \qquad (23)$$

4 Numerical solution

4.1 Procedure of numerical calculations

Numerical procedure to explicitly obtain solutions as an initial value problem is briefly summed up as follows.

(1) Using the flow rates given at the junctions as the initial values, $\Delta\alpha$, ΔP, $\dot{M}_{tE}$, $\dot{M}_{tC}$, Δh_g, Δh_l in the volumes after time increment Δt are calculated by using the solutions of simultaneous equations described in the section 2 in this chapter and state change equations in the section 3.2. Subsequently, equilibrium or non-equilibrium condition of each phase is determined as indicated in Fig. 1.

(2) On the other hand, using the thermodynamic states in the volumes and the flow rates at junctions as initial values $\Delta W_{g,J}$ and $\Delta W_{l,J}$, and $\Delta W_{g,K}$ and $\Delta W_{l,K}$ are calculated by using Eqs.(5) and (6), and Eqs.(19) and (20) respectively.

(3) New time step values are determined by adding the increments to the old time step values in the volume and at the junction.

(4) New time increment Δt is determined by the rates of states changes in volumes. This method is described in detail in the section 4.4.

4.2 Pressure, void fraction and enthalpy

Changes of pressure and void fraction in the volume are derived as follows.

By the total differentiation of mass which is calculated by using void fraction and density in the volume, we get

$$\Delta M_a = \left(\alpha_a^* \cdot \Delta\rho_a + \rho_a \cdot \Delta\alpha_a\right)V \qquad (a = g, l) \tag{24}$$

If we use $\alpha_a^* = \alpha_a + \Delta\alpha_a$, Eq.(24) expresses absolute conserved relation.

If we take ρ =f(P, h), then

$$\left.\begin{aligned} \Delta\rho_g &= R_1\Delta P + R_2\Delta h_g \\ \Delta\rho_l &= R_3\Delta P + R_4\Delta h_l \end{aligned}\right\} \tag{25}$$

Where

$$
\left.
\begin{aligned}
R_1 &= \left(\frac{\partial \rho_g}{\partial P}\right)_{hg}, \quad R_2 = \left(\frac{\partial \rho_g}{\partial h_g}\right)_P && \text{for } IQG = -1 \\
R_3 &= \left(\frac{\partial \rho_l}{\partial P}\right)_{hl}, \quad R_4 = \left(\frac{\partial \rho_l}{\partial h_l}\right)_P && \text{for } IQL = -1 \\
R_1 &= \left(\frac{d\rho_g}{dP}\right)_{sat}, \quad R_2 = 0 && \text{for } IQG = 1 \\
R_3 &= \left(\frac{d\rho_l}{dP}\right)_{sat}, \quad R_4 = 0 && \text{for } IQL = 1 \\
\left(\frac{\partial \rho}{\partial P}\right)_h &= \frac{\rho \kappa c_v + \beta}{c_P} \\
\left(\frac{\partial \rho}{\partial h}\right)_P &= \frac{-\rho\beta}{c_P}
\end{aligned}
\right\} \qquad (26)
$$

Substituting Eqs.(12)～(17) into the term Δh_a(a=g,l) of Eqs.(25) and after rearranging, we get

$$
\left.
\begin{aligned}
\Delta\rho_g &= SX1 \cdot \Delta P + SX3 \cdot \Delta t \\
\Delta\rho_l &= SX2 \cdot \Delta P + SX4 \cdot \Delta t
\end{aligned}
\right\} \qquad (27)
$$

Where

$$
\left.
\begin{aligned}
SX1 &= R_1 + R_2\left(\frac{1}{\rho_g} + \frac{C_7\, y_7}{M_g\, y_6}\right) \\
SX2 &= R_3 + R_4\left(\frac{1}{\rho_l} - \frac{C_8\, y_9}{M_l\, y_6}\right) \\
SX3 &= \frac{R_2}{M_g}\left(C_{10} + \frac{C_7 y_8}{y_6}\right) \\
SX4 &= C_{11} + C_9 \cdot \dot{M}_{ZC,K} - \frac{C_8 y_{10}}{y_6} \\
C_7 &= \left(h_{gs} - h_g\right)_K + C_5 \\
C_8 &= \left(h_{ls} - h_l\right)_K + C_5 \\
C_9 &= \left(h_g - h_l\right)_K + C_5
\end{aligned}
\right\} \qquad (28)
$$

For the calculation of these terms, it is necessary to calculate terms in the equations of state change in junction flow and in the volume described in the section 3.2 beforehand. Substituting Eq.(27) into the term $\Delta\rho_a$ of the right hand side of Eq.(24) and substituting Eqs.(1) and (2) into the left hand side of Eq.(24), and after rearranging, we get

$$SX5 \cdot \Delta P + \rho_g \Delta \alpha_g = SX7 \cdot \Delta t \tag{29}$$

$$SX6 \cdot \Delta P - \rho_l \Delta \alpha_g = SX8 \cdot \Delta t \tag{30}$$

Where

$$\left.\begin{aligned}
SX5 &= \alpha_g^* \cdot SX1 - \frac{y_{13}}{V} \\
SX6 &= \alpha_l^* \cdot SX2 + \frac{y_{13}}{V} \\
SX7 &= \frac{y_{12}}{V} - \alpha_g^* \cdot SX3 \\
SX8 &= \frac{y_{14}}{V} - \alpha_l^* \cdot SX4 \\
y_{11} &= \frac{1}{y_6}(y_8 + y_{10}) \\
y_{12} &= RHSCG - \dot{M}_{ZC,K} + y_{11} \\
y_{13} &= \frac{1}{y_6}(y_7 + y_9) \\
y_{14} &= RHSCL + \dot{M}_{ZC,K} - y_{11} \\
RHSCG &= W_{g,J-1} - W_{g,J} + (\dot{M}_{ZE} - \dot{M}_{ZC})_{J-1} \\
RHSCL &= W_{l,J-1} - W_{l,J} - (\dot{M}_{ZE} - \dot{M}_{ZC})_{J-1}
\end{aligned}\right\} \tag{31}$$

The solutions of simultaneous equations (29) and (30) are gotten as follows.

$$\Delta P = \frac{1}{SXY}(SX7 \cdot \rho_l + SX8 \cdot \rho_g)\Delta t \tag{32}$$

$$\Delta \alpha = \frac{1}{SXY}(SX7 \cdot SX6 - SX8 \cdot SX5)\Delta t \tag{33}$$

Where $SXY = SX5 \cdot \rho_l + SX6 \cdot \rho_g$

Then, enthalpy change of each phase Δh_g and Δh_l are obtained from Eqs.(12)～(15) and phase change rates are from Eqs.(16)～(18) .

4.3 Temperatures

Now, we know the pressure and enthalpy in the volume. Then, other thermodynamic states are determined by using the steam table as a function of pressure and enthalpy. However, as for temperatures, we can also evaluate them as a function of mass and enthalpy of each phase, as follows. The consistencies between variables which are obtained in different solution schemes are examined as described in the section 4.5.

If we express the temperatures as a function of mass and enthalpy of each phase,

then

$$T_a=f(M_g, M_l, H_g, H_l)$$

Where $H_a=M_a h_a$ (a=g,l).

Then
$$\Delta T_a = \frac{\partial T_a}{\partial M_g}\Delta M_g + \frac{\partial T_a}{\partial M_l}\Delta M_l + \frac{\partial T_a}{\partial H_g}\Delta H_g + \frac{\partial T_a}{\partial H_l}\Delta H_l \tag{34}$$

If we take $T_a=f(P, h_a)$, then

$$\left.\begin{aligned}
&\frac{\partial T_g}{\partial M_l}=\left(\frac{\partial T_g}{\partial P}\right)_{h_g}\cdot\frac{\partial P}{\partial M_l}\quad,\quad \frac{\partial T_l}{\partial M_g}=\left(\frac{\partial T_l}{\partial P}\right)_{h_l}\cdot\frac{\partial P}{\partial M_g}\\
&\frac{\partial T_g}{\partial H_l}=\left(\frac{\partial T_g}{\partial P}\right)_{h_g}\cdot\frac{\partial P}{\partial H_l}\quad,\quad \frac{\partial T_l}{\partial H_g}=\left(\frac{\partial T_l}{\partial P}\right)_{h_l}\cdot\frac{\partial P}{\partial H_g}\\
&\frac{\partial T_a}{\partial M_a}=\left(\frac{\partial T_a}{\partial P}\right)_{h_a}\left\{\frac{\partial P}{\partial M_a}-\left(\frac{\partial P}{\partial h_a}\right)_{T_a}\cdot\frac{\partial h_a}{\partial M_a}\right\}\\
&\frac{\partial T_a}{\partial H_a}=\left(\frac{\partial T_a}{\partial P}\right)_{h_a}\left\{\frac{\partial P}{\partial H_a}-\left(\frac{\partial P}{\partial h_a}\right)\cdot\frac{\partial h_a}{\partial H_a}\right\}
\end{aligned}\right\} \tag{35}$$

Where, the terms in Eq.(35) are given as

$$\left.\begin{aligned}
&\frac{\partial P}{\partial M_g}=\frac{\rho_l}{VD}\left\{1+\frac{h_g}{\rho_g}\left(\frac{\partial \rho_g}{\partial h_g}\right)_P\right\}\\
&\frac{\partial P}{\partial M_l}=\frac{\rho_g}{VD}\left\{1+\frac{h_l}{\rho_l}\left(\frac{\partial \rho_l}{\partial h_g}\right)_P\right\}\\
&\frac{\partial P}{\partial H_g}=\frac{-1}{VD}\frac{\rho_l}{\rho_g}\left(\frac{\partial \rho_g}{\partial h_g}\right)_P\\
&\frac{\partial P}{\partial H_l}=\frac{-1}{VD}\frac{\rho_g}{\rho_l}\left(\frac{\partial \rho_l}{\partial h_l}\right)_P\\
&\frac{\partial h_a}{\partial M_a}=\frac{-h_a}{M_a}\\
&\frac{\partial h_a}{\partial H_a}=\frac{1}{M_a}\\
&D=\left\{\alpha_g\rho_l\left(\frac{\partial \rho_g}{\partial P}\right)_{h_g}+\alpha_l\rho_g\left(\frac{\partial \rho_l}{\partial P}\right)_{h_l}\right\}
\end{aligned}\right\} \tag{36}$$

From the general expressions of thermodynamics, we get

$$\left.\begin{aligned}\left(\frac{\partial T}{\partial P}\right)_h &= \frac{T\beta - 1}{c_p \rho} \\ \left(\frac{\partial P}{\partial h}\right)_T &= \frac{\rho}{1 - T\beta} \\ \left(\frac{\partial \rho}{\partial h}\right)_p &= \frac{-\rho\beta}{c_p} \\ \left(\frac{\partial \rho}{\partial P}\right)_h &= \frac{\rho\kappa c_v + \beta}{c_P}\end{aligned}\right\} \qquad (37)$$

Thus, using Eqs.(34)～(37), Eqs.(1),(2),(12) and (13) we can evaluate the temperatures changes.

4.4 Time step control.

The basic idea of time step control is in judgment of the rates of state changes in the volume. We take pressure and mass of each phase as judging parameters to control time increment. New parameters are introduced as :

$CR_1 = \Delta P/P$, $CR_3 = \Delta M_g/M_g$, $CR_4 = \Delta M_l/M_l$, $CR_6 = (\Delta P(n) - \Delta P(n+1)) / \Delta P_m$ (ΔP_m is larger one of $|\Delta P(n)|$ and $|\Delta P(n+1)|$). Setting an upper and lower limits for these parameters, time step is controlled by the values of these parameters checking whether they exceed the limits or not. The limits for parameters CR_1, CR_3, CR_4 are set by CR_{min}, and the CR_{max}, and limits for parameter CR_6 are by CC_{min}, and CC_{max}. These limits are given by input data for code running.

Using the maximum value of each parameter in all volumes, time step (Δt) is controlled as follows.

(1) If one of $|CR_1|$, $|CR_3|$ and $|CR_4|$ exceeds CR_{max}, Δt is multiplied by 1/2.

(2) If all of $|CR1|$, $|CR_3|$ and $|CR_4|$ are less than CR_{min} and $|CR_6|$ is less than CC_{min}, Δt is multiplied by 1.25.

(3) If in any volume, $|CR_3|$ or $|CR_4| > CR_{min}$ and $|CR_6| > CC_{max}$ occur simultaneously, Δt is multiplied by 1/2.

(4) If $CR_{min} < |CR_3|$ and $|CR_4| < CR_{max}$ and $|CR_6| < CC_{min}$ occur simultaneously, and all of $|CR_1 \cdot 2|$, $|CR_3 \cdot 2|$ and $|CR_4 \cdot 2|$ are less than CR_{max}, Δt is multiplied by 1.25.

Controlling method mentioned above is defined empirically as of the present. It may be revised to a better one in the future.

4.5 Examination method of consistencies between variables obtained by numerical calculation

Thermodynamic states of each phase in the volume can be obtained by two different solution schemes using basic equations and general expressions of thermodynamic. So, we can examine the correctness of overall numerical calculation method by comparing the state values obtained by two different solution schemes in the calculation of the non-equilibrium two-phase flow. Further it is also necessary to confirm no accumulation of error occurs in mass or energy by checking that the summation of the total mass or energy dealt with in a whole calculation model is conserved at any time during the calculation.

First we have already obtained the state values of pressure P, void fraction α and enthalpy of each phase h_g, h_l by using the equations of mass conservation and the first law of thermodynamics of each phase, simultaneously, as described before in this chapter.

On the other hand, mass change of each phase is directly calculated by mass conservation equation of each phase Eq.(1) and Eq.(2).

Therefore the density of each phase ρ_g, ρ_ℓ is calculated using mass of each phase and void fraction α. Further, temperature change of each phase is obtained from Eq.(34) with the general expressions of thermodynamics Eq.(35)～ Eq.(37) as a totaled effect of changes of mass and enthalpy of each phase.

Then, from the steam table as a function of P and h_g or h_ℓ ,density ρ_{gST} and temperature T_{gPU} of gas or $\rho_{\ell ST}$ and $T_{\ell PU}$ of liquid are obtained, respectively. Saturated temperature T_s of pressure P is also obtained. Thus, we can compare ρ_g, ρ_ℓ with ρ_{gST} , $\rho_{\ell ST}$ and T_g,T_ℓ with T_{gPU}, $T_{\ell PU}$ respectively.

The specific enthalpy of each phase is obtained also from the total energy conservation equation in the volume as follows.

The internal energy in the Volume K is defined as

$$E_a = (M_a e_a)_K \qquad (a = g, \ell) \tag{38}$$

The change of the kinetic energy in the Volume K is expressed as

$$\frac{\Delta}{\Delta t}\left(M_a \frac{u_a^2}{2}\right)_K = (\Delta Z \cdot u_a)_K \frac{\Delta W_{a,K}}{\Delta t} - \frac{1}{2} u_{a,K}^2 \frac{\Delta M_{a,K}}{\Delta t} \tag{39}$$

Substituting Eqs.(38) and (39) into energy conservation equations (3) and (4), we can get ΔE_aas a function of ΔW_a and ΔM_a. The term ΔW_a is obtained from Eqs.(12) and

(13) and the term ΔM_a is from Eqs.(1) and (2) using Eqs.(19) and (20) of this report and using Eq.(20)～Eq.(23) of the previous report[1]. The internal energy E_a is obtained by integration of every increment ΔE_a and the specific internal energy is determined by using $e_{aE}=E_a/M_a$. The specific enthalpy is therefore obtained using the relation $H_{aST}=e_{aE}+P/\rho_a$.

Thus, we can compare h_g and h_ℓ obtained from the relational expressions of thermodynamic state change, with h_{gST} and $h_{\ell ST}$ obtained from total energy conservation equations respectively.

Further, conservation of mass and energy in the calculation of flow behavior from volume to volume is examined as follows.

The mass and energy in the test pipe are changing due to inflow to and outflow from the test pipe. However, the total ones contained in the test pipe and (integrated values of outflow)－(integrated values of inflow) should be conserved at any time.

If the thermodynamic states obtained in the two different ways mentioned above coincide with each other, and conservation of mass and energy of each phase is confirmed through the examinations above, it will prove that the numerical calculation method for general condition of unsteady two-phase flow with non-equilibrium states is correct in evaluating the thermodynamic states.

5. Some examples of numerical calculation results.

In order to verify the validity of numerical calculation of non-equilibrium two-phase flow, calculations are made for each type of non-equilibrium conditions classified in Table.1 by selecting the initial and boundary conditions.

5.1 Non-equilibrium conditions of saturated vapor and subcooled water two-phase flow.(Case. 1)

The test pipe dimensions are about 73mm diameter and 4.1m length. The test pipe is divided into eight sections of equal control volume and provided by boundary junction which supply water flow to the control volume of number 1 and boundary volume which gives the boundary condition for the flow from volume number 8 for the numerical calculation by the volume-junction model as shown in Fig.2.

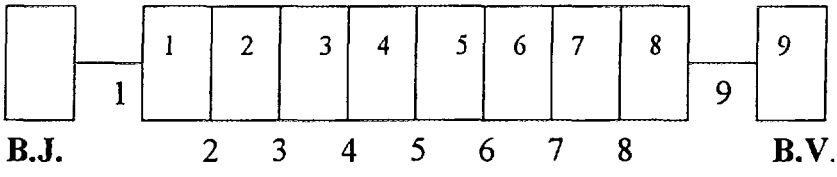

Fig.2 Control volume for non-equilibrium two-phase flow.

For the initial condition, slight superheated vapor of 2.0MPa 488.3K (saturated temperature is 485.57K) and subcooled water of 463.2K are uniformly filled with void fraction α_0=0.95 in the test pipe. At the start of calculation, subcooled water with specific enthalpy 807.5kJ/kg (corresponds to 2.0MPa, 462.5K) is supplied to liquid phase of Vol.1 by the flow rate of 10kg/s from Boundary Junction 1 with the pressure of Boundary Volume, 1.5MPa. Then, unsteady non-equilibrium two-phase flow of subcooled water and saturated vapor takes place in the test pipe with pressure decreasing due to vapor and water discharge.

Calculated results are shown in Fig.3～Fig.11. Pressure behaviors in Fig.3 show that decreasing pressure originated in Vol.8 is propagated upstream. Cold water injected into Vol.1 decrease the pressure at the part less than the downstream pressure after 0.01 sec. Vapor velocities at junctions decrease rapidly as shown in Fig.6 due to a reversed pressure profile along the flow. But liquid velocities at junctions continue to increase a little while as shown in Fig.7 due to larger momentum in the liquid flow than in the vapor flow. Especially the velocity $V_{lj}(2)$ continues to increase even after 0.02 sec. This is because the constant liquid flow rate from Boundary Junction is given at the inlet junction to Volume 1. The velocity $V_{lj}(1)$ is determined by using the flow

area of the downstream volume. The $V_{IJ}(1)$ is about 50 $^{m}/_{s}$ for the initial condition, which causes the increasing flow rate in the downstream even after the occurrence of reversed pressure profile along the flow at 0.01 sec. The similar changes of velocities in volumes are shown in Figs.8 and 9, too.

Temperatures of vapor are shown in Fig.4 in terms of T_g, T_{gPU} and T_s. It shows that superheated vapor becomes saturated soon after the transient calculation starts due to pressure decrease. Temperatures of liquid are shown in Fig.5 in terms of T_ℓ and $T_{\ell PU}$ which indicate the slight temperature rise by 0.2～0.3k due to condensation of saturated vapor.

Agreements of T_g and T_{gPU} are very exact and after vapor became saturated, agreements of T_g and T_s are also very exact. Agreements of T_ℓ and $T_{\ell PU}$ are very exact showing that liquid is always subcooled. Specific enthalpies of each phase in some volumes are shown Fig.10 in terms of h_g and h_{gST}, and in Fig.11 in terms of h_ℓ and $h_{\ell ST}$ respectively. Agreements of h_g and h_{gST}, and of h_ℓ and $h_{\ell ST}$ are very exact respectively. Densities of each phase in some volumes are shown in Fig.12 in terms of ρ_g and ρ_{gST}, and in Fig.13 in terms of ρ_ℓ and $\rho_{\ell ST}$ respectively.

Agreements of ρ_g and ρ_{gST}, and of ρ_ℓ and $\rho_{\ell ST}$ are very exact respectively.

Conservation of mass and energy of each phase is shown in Figs.14 and 15 in terms of TOTMG, TOTML, TOTM, TOTEG, TOTEL and TOTE. These figures show very strict conservation of total mass and total energy at any time, respectively. Numerical results show that each value of TOTM and TOTE are 0.458747kg and 516.232kJ, respectively at the start of calculation and they are 0.458747kg and 516.235kJ, respectively at the end of calculation.

5.2 Non-equilibrium condition of superheated vapor and saturated water. (Case.2)

Noding of test pipe for numerical calculation is identical with Fig.2 in this case, too.

For the initial condition, saturated two-phase fluids of 2.0MPa are filled with void fraction α_0=0.95 in the test pipe. At the start of calculation superheated vapor with specific enthalpy 3,025.0kJ/kg (corresponds to 2.0MPa, 573.2K) is supplied to vapor phase of Vol.1 by the flow rate of 2kg/s from Boundary Junction 1 with the pressure of Boundary Volume is 2.0MPa. Then, unsteady non-equilibrium two-phase flow of superheated vapor and saturated water takes place in the test pipe.

Calculated results are shown in Fig.16～Fig.28. Pressure behavior in Fig.16 show that increasing pressure originated in Vol.1 due to injection of superheated vapor is

propagated downstream. Then discharge flow from Vol.8 starts and it causes pressure decrease of Vol.8 being propagated upstream. Temperatures of each phase in Vol. 4 are shown in terms of T_g, T_{gPU} and T_s in Fig.17, and in terms of T_ℓ, $T_{\ell PU}$ and T_s in Fig.18, respectively. Vapor is going to be superheated and the liquid becomes a subcooled state caused by the first pressure increase. After that, pressure decreases rapidly and liquid becomes saturated. However vapor temperatures increase due to the inflow of superheated vapor from Boundary Junction. Agreements of T_g and T_{gPU}, and of T_ℓ and $T_{\ell PU}$ are very exact respectively. Agreements of T_ℓ and T_s are also very exact, after liquid became saturated. Vapor velocities at Junctions become uniform throughout the test pipe at 0.05sec. However liquid velocities at Junctions decrease a little as shown in Figs.19 and 20 because interfacial frictional force per unit volume of liquid decreases a little due to the increase of void fraction. Vapor velocities in volumes change similarly to those of junctions as shown in Fig.21. Liquid velocities in volumes are also similar to these of junctions except the velocity in Vol.1. As for the liquid in Vol.1, the acceleration force is given by only condensed vapor in Vol.1, since the pressure difference between upstream volume is zero. So, the velocity in Vol.1 $V_{IV}(1)$ increases very slowly as shown in Fig.22. Specific enthalpies of each phase in some volumes are shown in Fig.23 in terms of h_g and h_{gST}, and in Fig.24 in terms of h_ℓ and $h_{\ell ST}$ respectively. Agreements of h_g and h_{gST}, and of h_ℓ and $h_{\ell ST}$ are very exact respectively. Densities of each phase in some volumes are shown in Fig.25 in terms of ρ_g and ρ_{gST}, and in Fig.26 in terms of ρ_ℓ and $\rho_{\ell ST}$ respectively. Agreements of ρ_g and ρ_{gST}, and of ρ_ℓ and $\rho_{\ell ST}$ are very exact respectively.

Conservation of mass and energy of each phase is shown in Figs.27 and 28 respectively. These figures show very strict conservation of total mass and total energy at any time respectively. Numerical results show that each value of TOTM and TOTE are 0.4479755kg and 382.2645kJ, respectively at the start of calculation and they are 0.447976kg and 382.397kJ, respectively at the end of calculation.

5.3 Non-equilibrium condition of superheated vapor and subcooled water. (case.3)

To realize a non-equilibrium condition of this type, two kind of Boundary Junction are provided for the former test pipe with a Boundary Volume as shown in Fig.29.

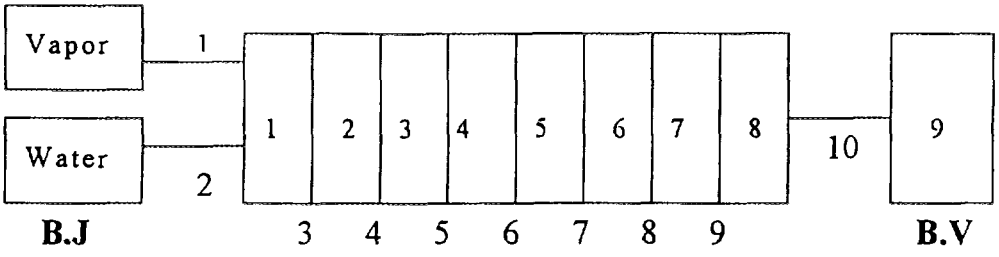

Fig.29 Control volume for superheated vapor and subcooled water two-phase flow.

For the initial condition, slightly superheated vapor of 2.0MPa, 488.3K and subcooled water 371.5K are uniformly filled with void fraction α_0=0.95 in the test pipe. At the start of calculation, superheated vapor with specific enthalpy 2,820kJ/kg (corresponds to 2.0MPa, 493.2K) is supplied to the vapor phase of Vol.1 by the flow rate of 3.2kg/s from Boundary Junction 1 and subcoled water with specific enthalpy 2,110kJ/kg (corresponds to 2.0MPa, 323.2K) is supplied to liquid phase of Vol.1 by the flow rate of 10kg/s from Boundary Junction 2. Pressure of Boundary Volume is 1.5MPa in this case. Then, unsteady non-equilibrium two-phase flow of superheated vapor and subcooled water take place in the test pipe.

Calculated results are shown in Fig.30～Fig.43. Pressure behaviors in Figs. **30-1, 2** shows that increasing pressure originated in Vol.1 due to injection of superheated vapor and subcooled water is propagated downstream. On the other hand, decreasing pressure originated in Vol.8 due to the flowing out to Boundary Volume is propagated upstream. Vapor temperature in Vol.4 is shown in Fig.31 in terms of T_g and T_s which indicate the appearance of superheated vapor from saturated state after 0.03sec. The temperature of each phase in Vol.1,4,8 are shown in Fig.32 in terms of T_g and T_{gPU}, and in Fig.33 in terms of T_ℓ and $T_{\ell PU}$ respectively. These temperatures show that vapor phase changes to superheated from saturated and liquid phase is kept subcooled.

Agreements of T_g and T_{gPU}, and of T_ℓ and $T_{\ell PU}$ are very exact respectively. Each flow of vapor and liquid in the test pipe starts at the inlet and outlet simultaneously and is propagated downstream and upstream respectively. Uniform flow at junctions are attained at about 0.04sec as shown in Figs.34 and 35. The flow in volumes are about the same as junction flow as shown in Fig.36 and 37. Specific enthalpies of each phase in some volumes are shown in Fig.38 in terms of h_g and h_{gST}, and in Fig.39 in terms of h_ℓ and $h_{\ell ST}$ respectively. Agreements of h_g and h_{gST}, and of h_ℓ and $h_{\ell ST}$ and are very exact respectively. Densities of each phase in some volumes are shown in

Fig.40 in terms of ρ_g and ρ_{gST}, and in Fig.41 in terms of ρ_ℓ and $\rho_{\ell ST}$ respectively.

Agreements of ρ_g and ρ_{gST}, and of ρ_ℓ and $\rho_{\ell ST}$ are very exact respectively. Conservation of mass and energy of each phase is shown in Figs.42 and 43. These figures show very strict conservation of total mass and total energy at any time respectively. Numerical results show that each value of TOTM and TOTE are 0.4947715kg and 516.232kJ, respectively at the start of calculation and they are 0.494772kg and 516.235kJ, respectively at the end of calculation.

6. Conclusion

(1) General basic expressions of unsteady non-equilibrium two-phase flow for numerical calculation by the volume-junction model are presented.

(2) Numerical method to explicitly obtain solutions for various kinds of non-equilibrium conditions in the volume and in the junction flow are presented

(3) Verification calculations for the validity of numerical method are made for each type of non-equilibrium conditions in the volume. The results show that each thermodynamic states of enthalpy, density and temperature of each phase which are obtained in the two different solution schemes coincide with each other and no accumulation of error in mass and energy was found.

It will prove that numerical calculation method for general condition of unsteady two-phase flow with non-equilibrium states functioned correctly in evaluating the thermodynamic state.

References

1. M. OKAZAKI, "Simple and Rational Numerical Method of two-phase Flow by the Use of Volume-Junction model,(I) Verification Calculation for Saturated Condition, "

2. M. OKAZAKI, "Development of two-phase Flow Analysis Code by 2V2T Model, (I) Derivation of Basic Equations," J. Nucl. Sci. Technol., 23[5], pp433-450 (1986)

[NOMENCLATURE]

A : Flow area

c_p : Isobaric specific heat capacity

c_v : Isochoric specific heat capacity

d_h : Hydraulic diameter

E : Internal energy

e : Specific internal energy

ΔF : Frictional force acting on the fluid in a volume

g : Gravitational acceleration

h : Specific enthalpy

h_{gST}, h_{lST} : Specific enthalpies of vapor and liquid which are given from steam table by pressure and temperature of each phase, respectively.

IQG, IQL : State flag in Volume. 1=saturated, -1=superheated or subcooled

L : Length of Volume

M : Mass

$\dot{M}_{tE}$: Evaporation rate due to pressure decreasing in a volume

$\dot{M}_{tC}$: Condensation rate due to pressure decreasing in a volume

$\dot{M}_{ZE}$: Evaporation rate due to pressure decreasing in a junction flow

$\dot{M}_{ZC}$: Condensation rate due to pressure decreasing in a junction flow

P : Pressure

Q_{cond} : Heat transfer rate due to condensation of vapor to liquid by temperature difference.

Δq^0_{Eg} : External heat added to a unit mass of gas in a volume

Δq^0_{El} : External heat added to a unit mass of liquid in a volume

$\Delta q'_{Eq}, \Delta q'_{El}$: Terms which define distribution of interphase frictional heat to gas or liquid phase

Δq_{jg} : Frictional heat added to a unit mass of gas phase in a junction flow

Δq_{jl} : Frictional heat added to a unit mass of liquid phase in a junction flow

Δq_{jig} : Of Δq_{fg}, interphase frictional heat

Δq_{fil} : Of Δq_{fl}, interphase frictional heat

Δq_{fpcg} : Of Δq_{fg}, frictional heat caused by phase change due to different velocities between phases

Δq_{fpcl} : Of Δq_{fl}, frictional heat caused by phase change due to different velocities between phases

Δq_{mg} : Mixing frictional heat in gas phase caused by incoming fluid flow to a volume

Δq_{ml} : Mixing frictional heat in liquid phase caused by incoming fluid flow to a volume

Δq_{TPg} : Heat added to a unit mass of gas phase

Δq_{TPl} : Heat added to a unit mass of liquid phase

ΔQ^0_{Eg} : External heat added to gas in a volume

ΔQ^0_{El} : External heat added to liquid in a volume

r : Latent heat

T_{gPU}, T_{lPU} : Temperatures of vapor and liquid which are given from steam table by pressure and enthalpy of each phase, respectively.

T : Temperature

t : Time

TOTML : Total mass of liquid including discharged one

TOTMG : Total mass of gas including discharged one

TOTM : (TOTML+TOTMG)/2

TOTEL : Total internal energy of liquid including discharged one

TOTEG : Total internal energy of gas including discharged one

TOTE : (TOTEL+TOTEG)/2

u : velocity

v : Specific volume

V : Volume

W : Mass flow rate

w : Phase change rate in a unit length of flow

α	:	Void fraction
β	:	Coefficient of thermal expansion
κ	:	Isothermal compressibility
η	:	Fraction of interphase friction heat distributed to gas phase
(subscript)		
θ	:	Angle between flow direction and vertical axis (θ =0 for upward vertical flow)
ρ	:	Density
ρ_{gST} , ρ_{lST}	:	Densities of vapor and liquid which are given from stream table by pressure and enthalpy of each phase, respectively.
c	:	Continuous phase
g	:	Gas phase
l	:	Liquid phase
gs	:	Saturated state of gas
ls	:	Saturated state of liquid
s	:	Saturated
t	:	Time
Z	:	Spacial
Wg	:	Effect of wall to gas
Wl	:	Effect of wall to liquid
gl	:	Gas phase affected by liquid phase
lg	:	Liquid phase affected by gas phase

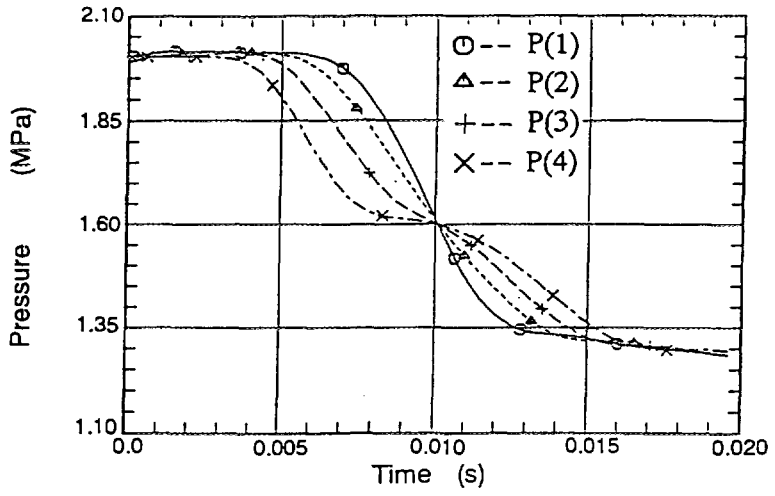

Fig.3-1 Pressure behavior of saturated vapor and subcooled two-phase flow (case.1)

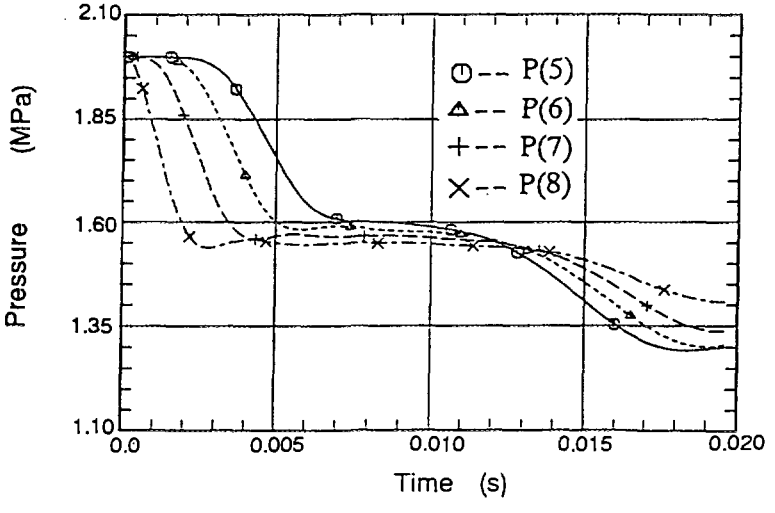

Fig.3-2 Pressure behavior of saturated vapor and subcooled two-phase flow (case.1)

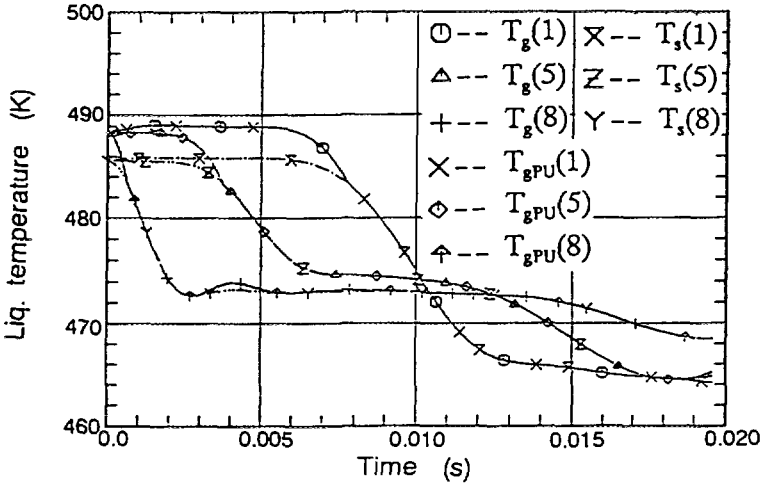

Fig.4 Comparison of vapor temperatures in Vol.1,5,8 (case.1)

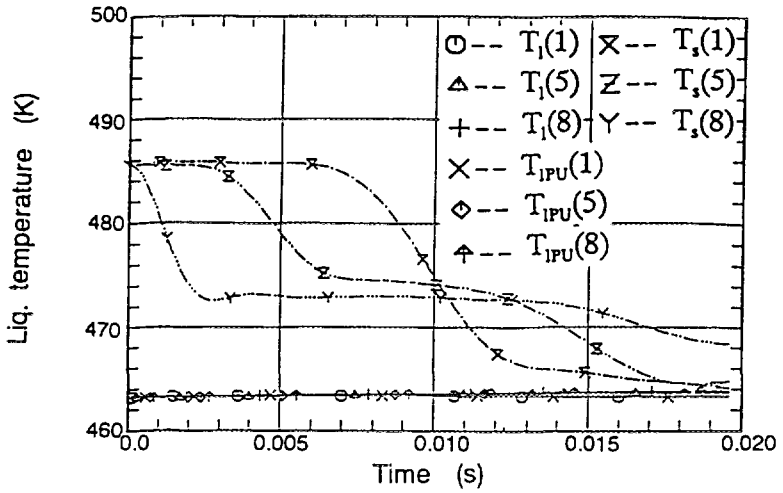

Fig.5 Comparison of liquid temperatures in Vol.1,5,8 (case.1)

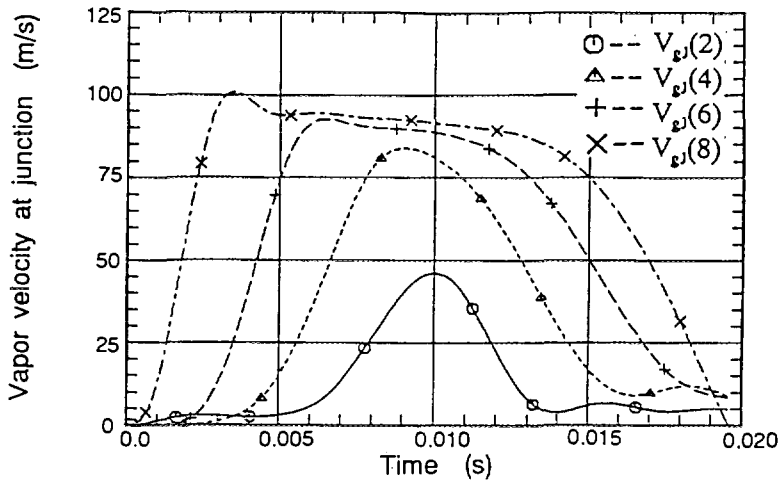

Fig.6 Vapor velocities at Junction 2,4,6,8 (case.1)

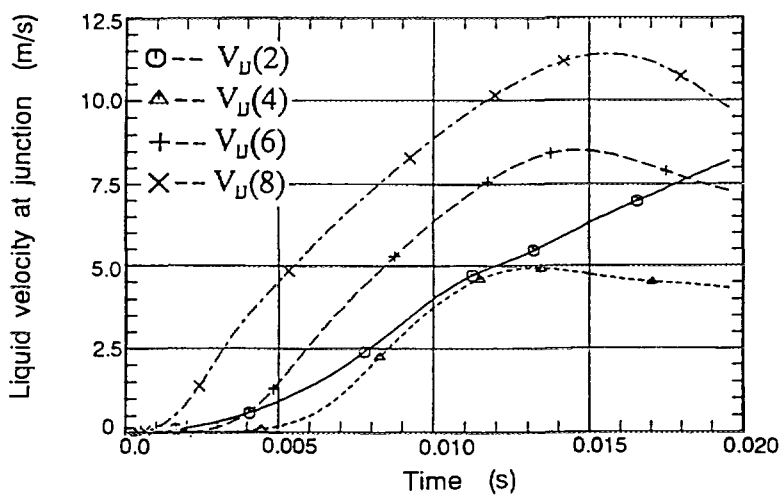

Fig.7 Liquid velocities at Junction 2,4,6,8 (case.1)

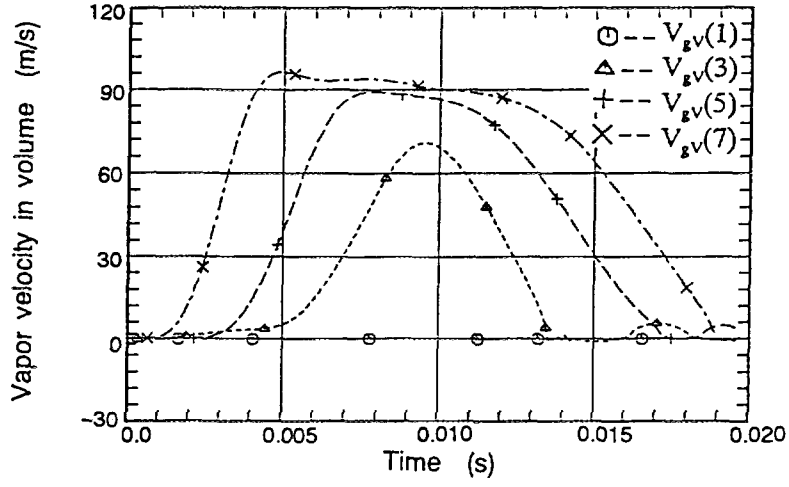

Fig.8 Vapor velocities in Volume 1,3,5,7 (case.1)

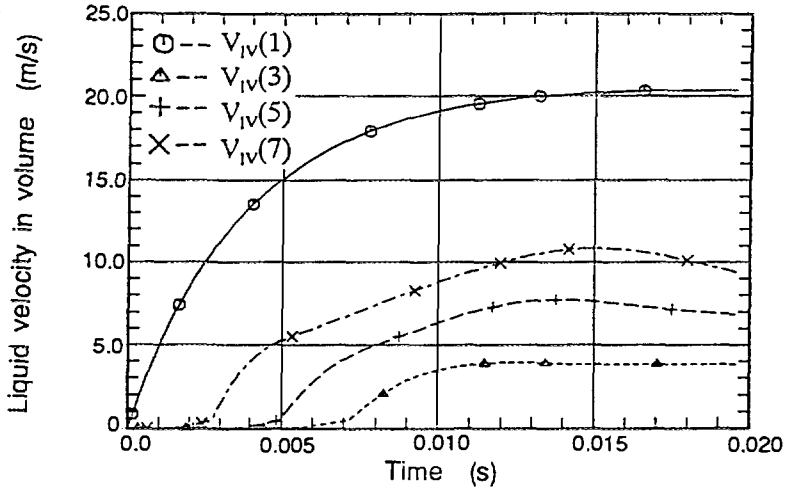

Fig.9 Liquid velocities in Volume 1,3,5,7 (case.1)

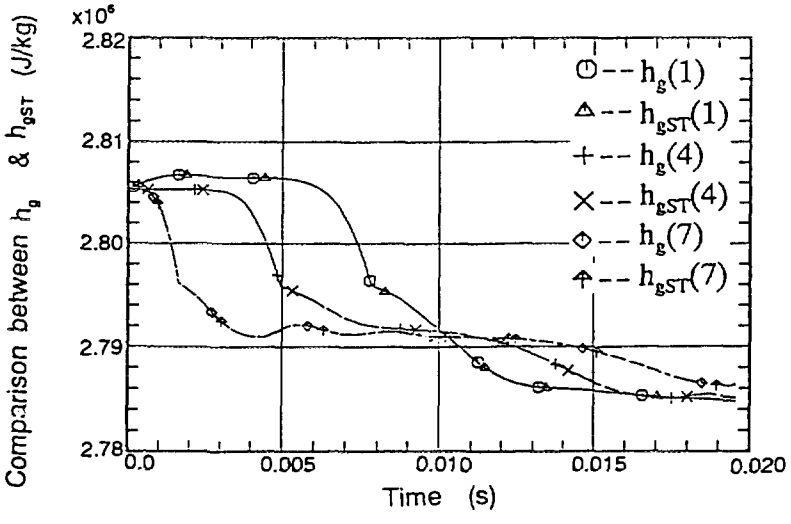

Fig.10 Comparison of specific vapor enthalpies in Volume 1,4,7 (case.1)

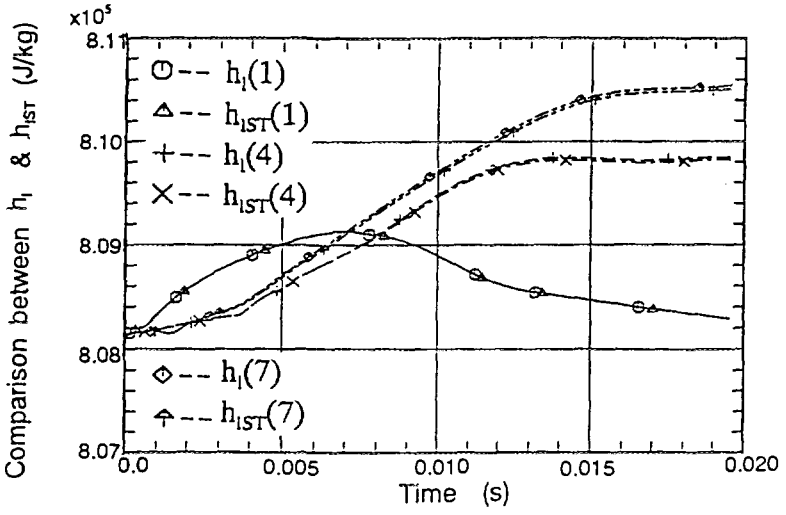

Fig.11 Comparison of specific liquid enthalpies in Volume 1,4,7 (case.1)

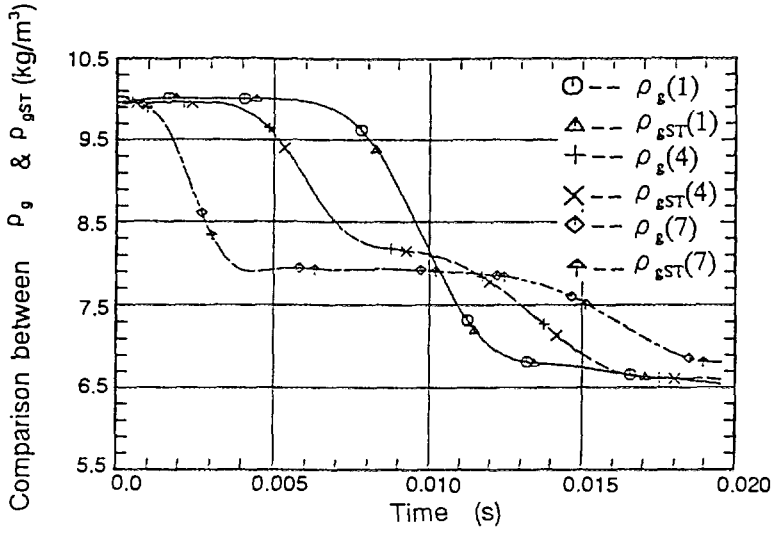

Fig.12 Comparison of vapor densities in Volume 1,4,7 (case.1)

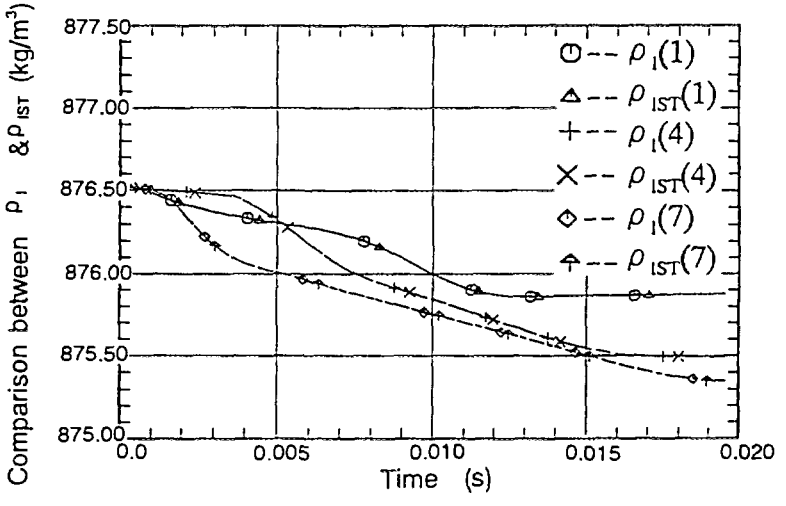

Fig.13 Comparison of liquid densities in Volume 1,4,7 (case.1)

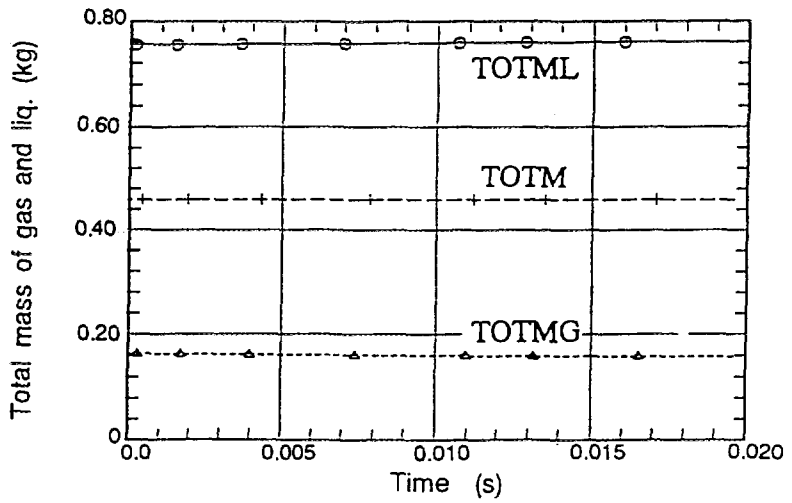

Fig.14 Total mass of vapor and liquid including discharged one. (case.1)

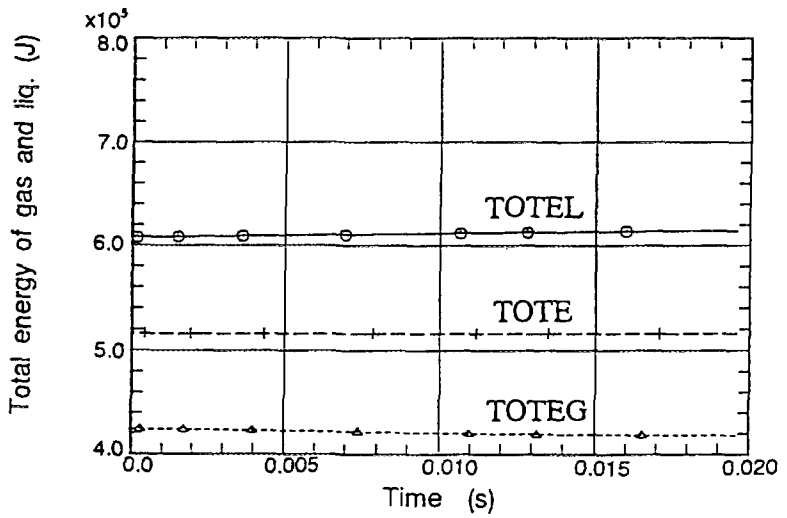

Fig.15 Total energy of vapor and liquid including discharged one. (case.1)

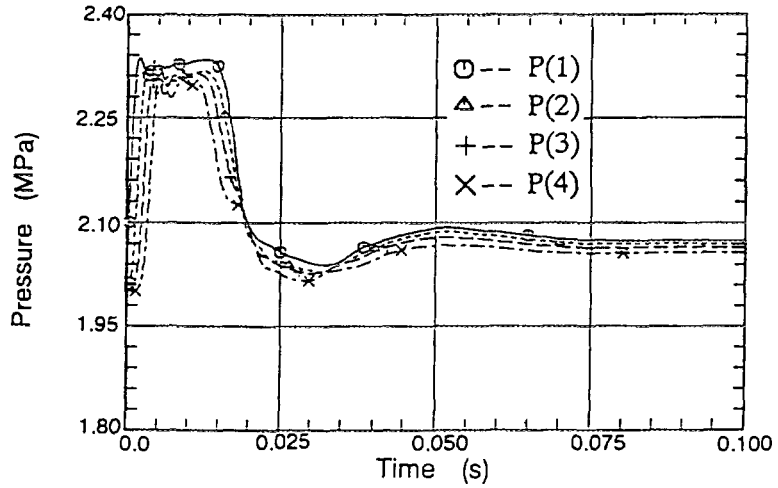

Fig.16-1 Pressure behavior of superheated vapor and saturated water two-phase flow (case.2)

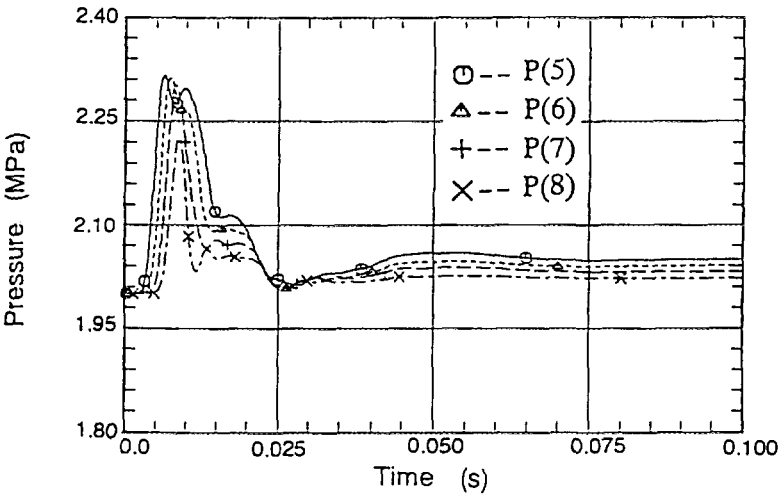

Fig.16-2 Pressure behavior of superheated vapor and saturated water two-phase flow (case.2)

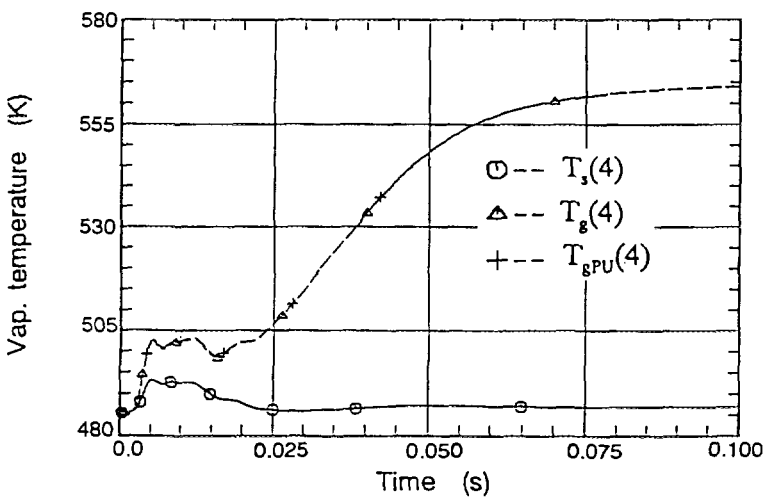

Fig.17 Comparison of vapor temperatures in Vol.4 (case.2)

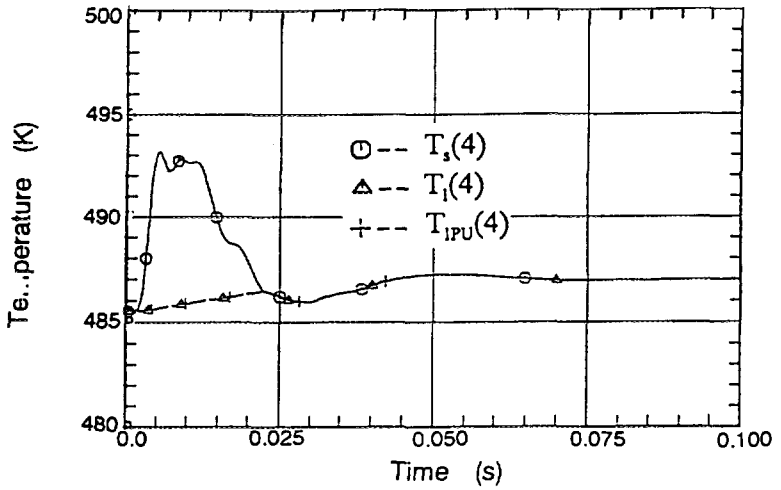

Fig.18 Comparison of liquid temperatures in Vol.4 (case.2)

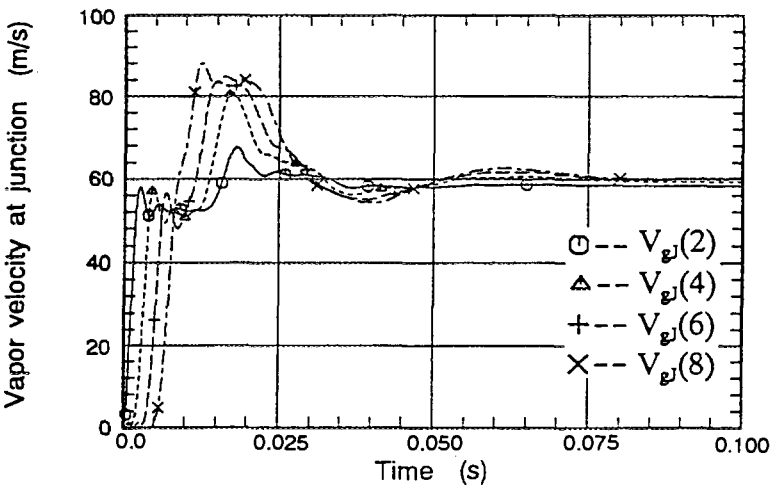

Fig.19 Vapor velocities at Junction 2,4,6,8 (case.2)

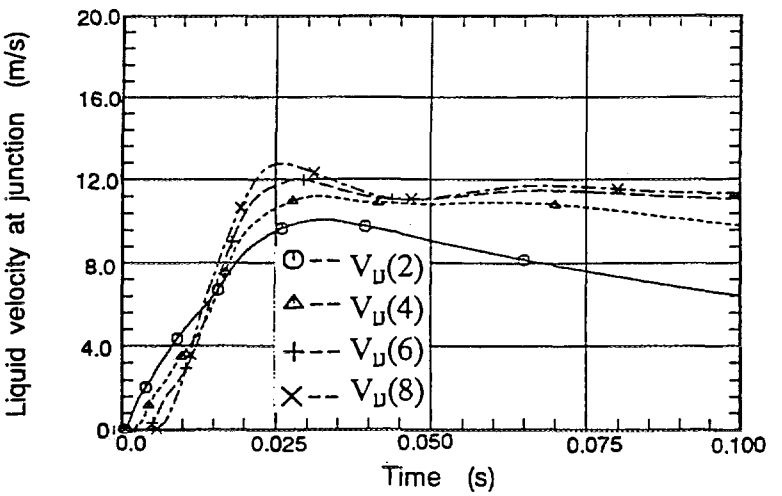

Fig.20 Liquid velocities at Junction 2,4,6,8 (case.2)

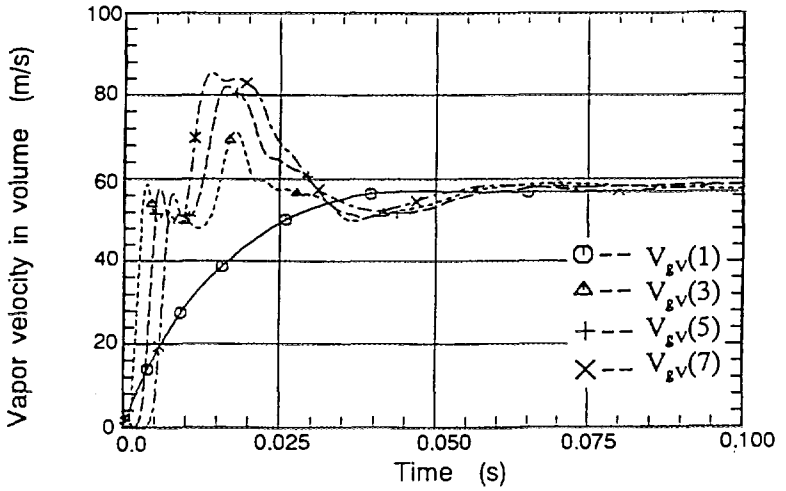

Fig.21 Vapor velocities in Volume 1,3,5,7 (case.2)

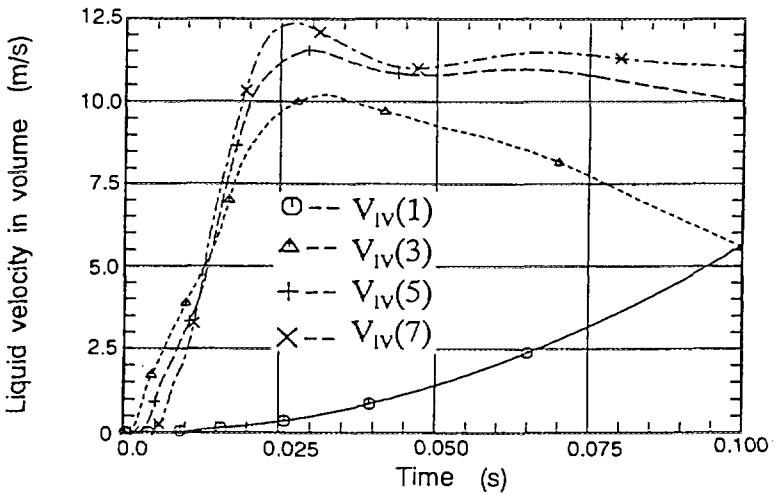

Fig.22 Liquid velocities in Volume 1,3,5,7 (case.2)

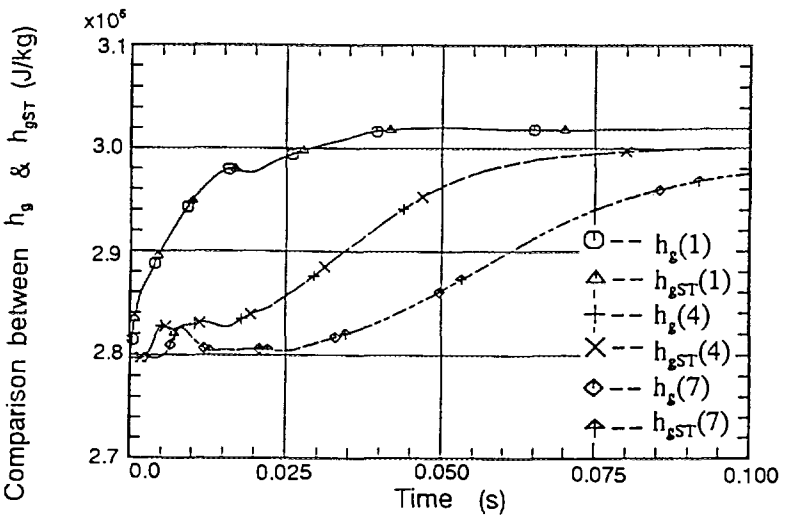

Fig.23 Comparison of specific vapor enthalpies in Volume 1,3,5,7 (case.2)

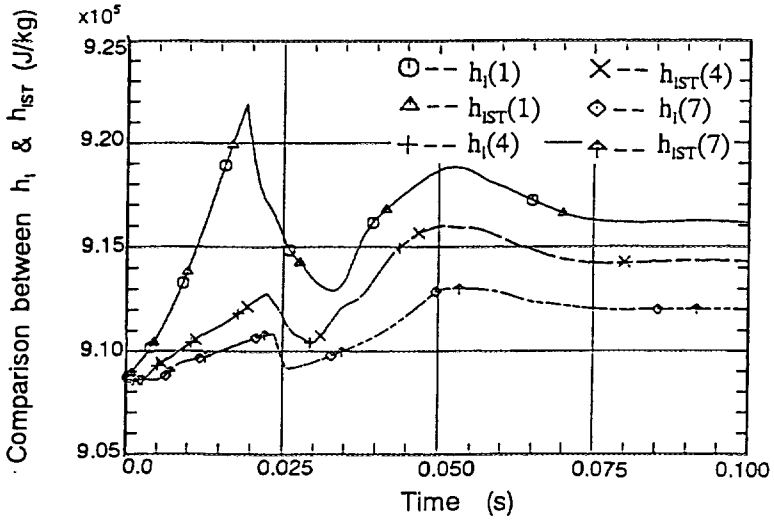

Fig.24 Comparison of specific liquid enthalpies in Volume 1,3,5,7 (case.2)

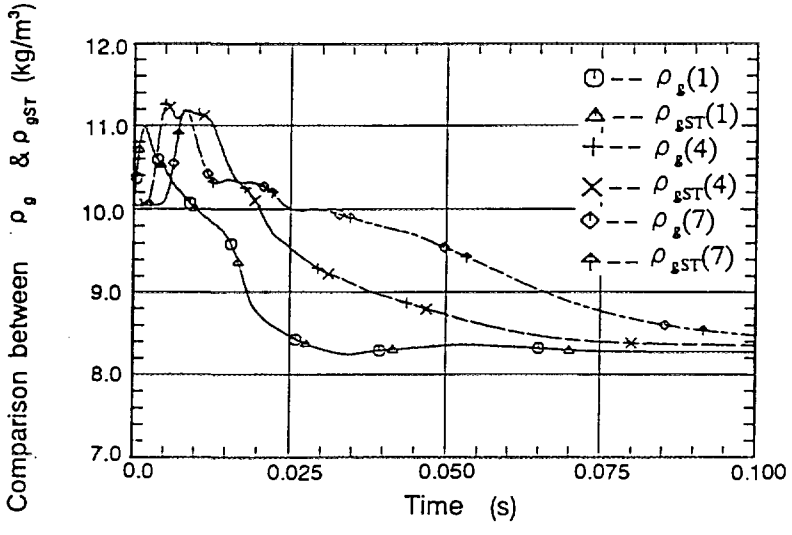

Fig.25 Comparison of vapor densities in Volume 1,4,7 (case.2)

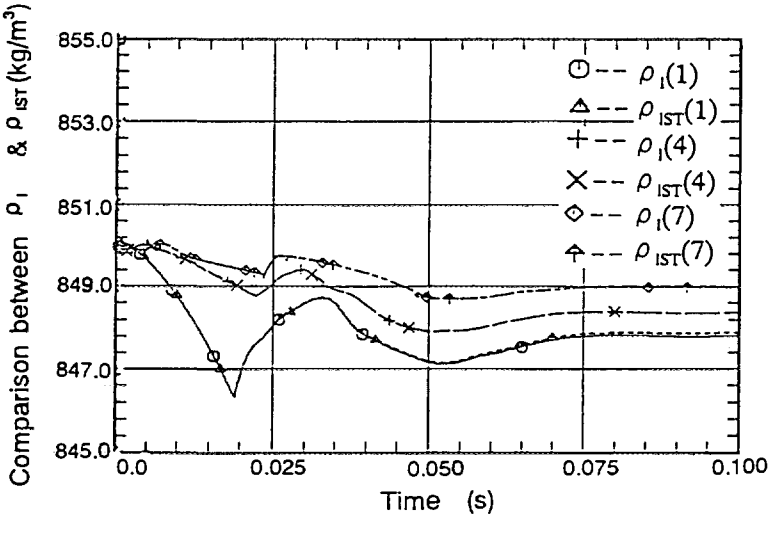

Fig.26 Comparison of liquid densities in Volume 1,4,7 (case.2)

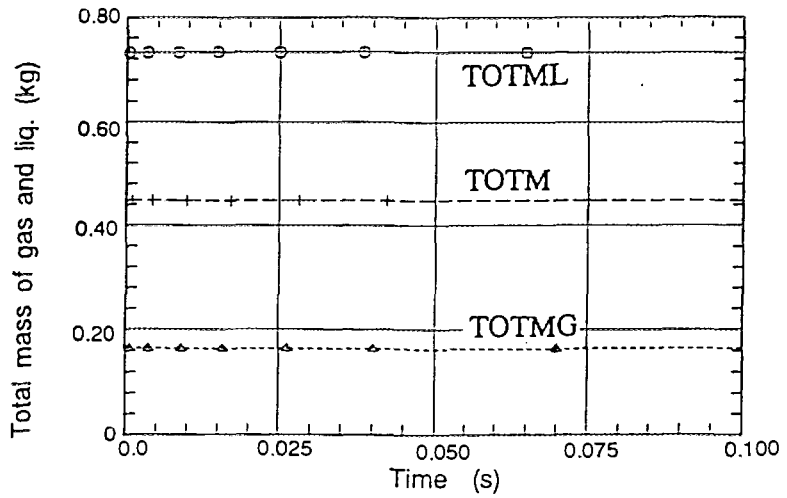

Fig.27 Total mass of vapor and liquid including discharged one. (case.2)

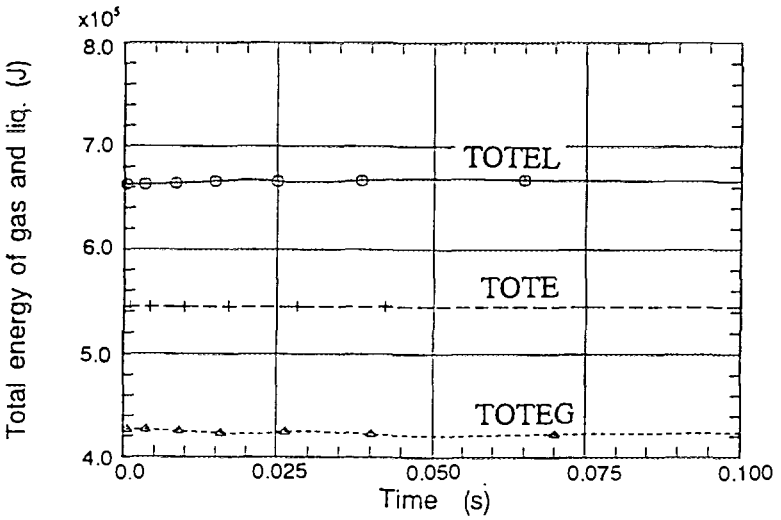

Fig.28 Total energy of vapor and liquid including discharged one. (case.2)

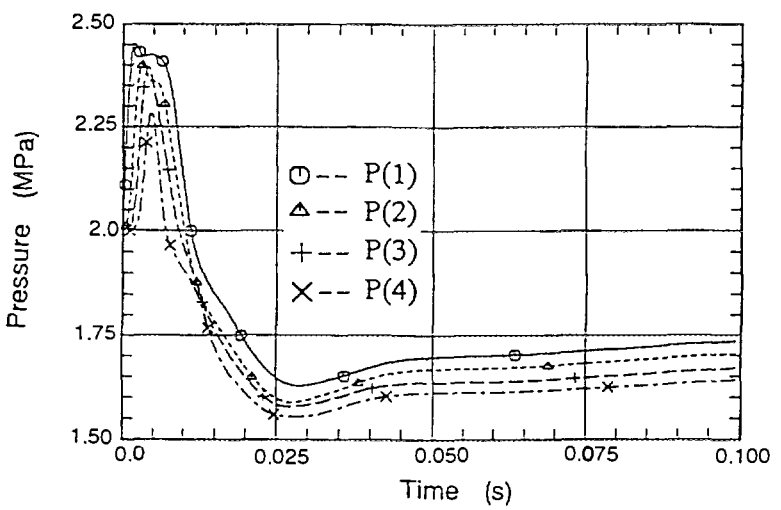

Fig.30-1 Pressure behavior of superheated vapor and subcooled water two-phase flow (case.3)

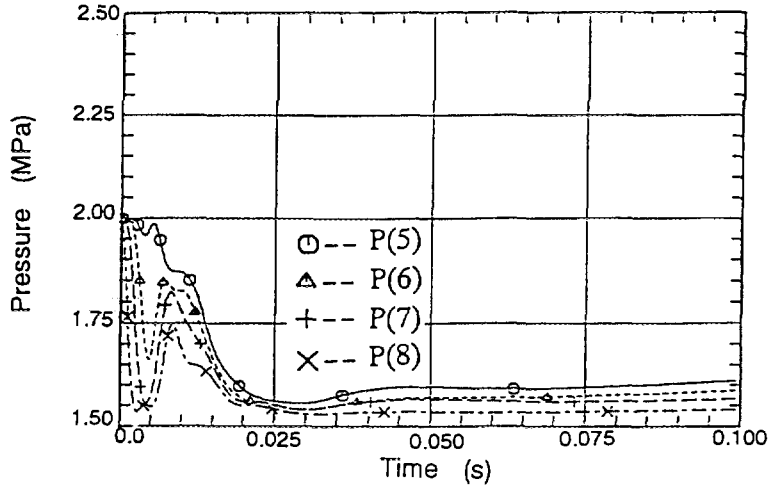

Fig.30-2 Pressure behavior of superheated vapor and subcooled water two-phase flow (case.3)

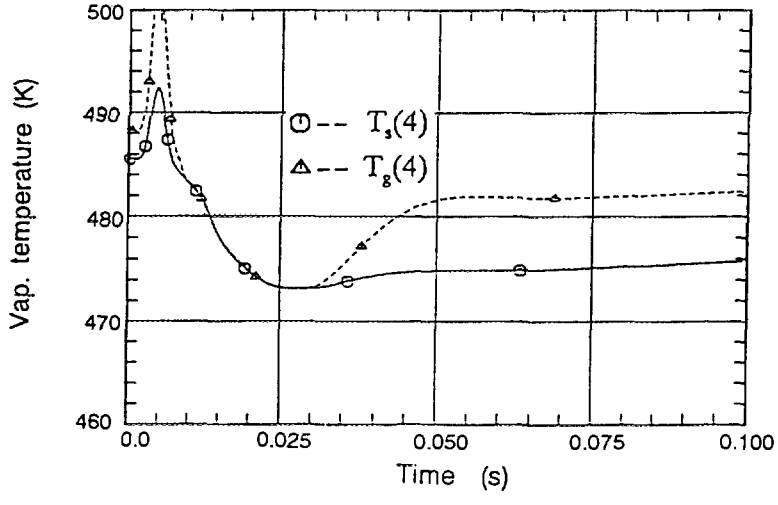

Fig.31 Vapor temperature in Vol.4 (case.3)

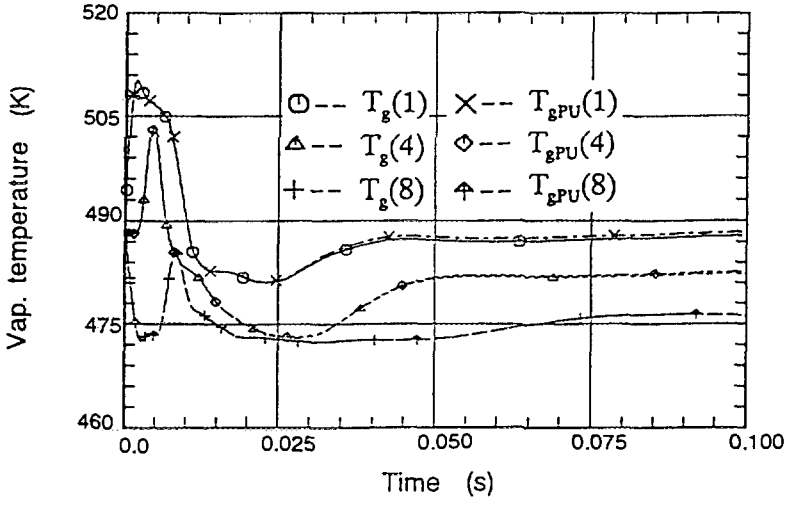

Fig.32 Comparison of vapor temperatures in Vol. 1,4,8 (case.3)

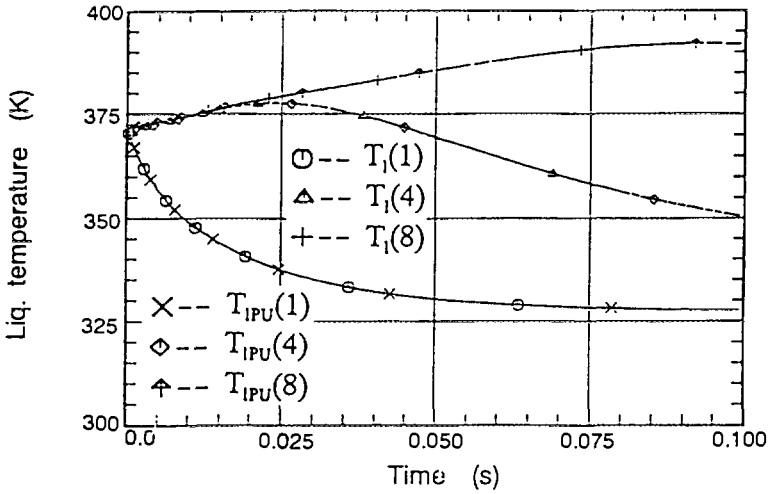

Fig.33 Comparison of liquid temperatures in Vol. 1,4,8 (case.3)

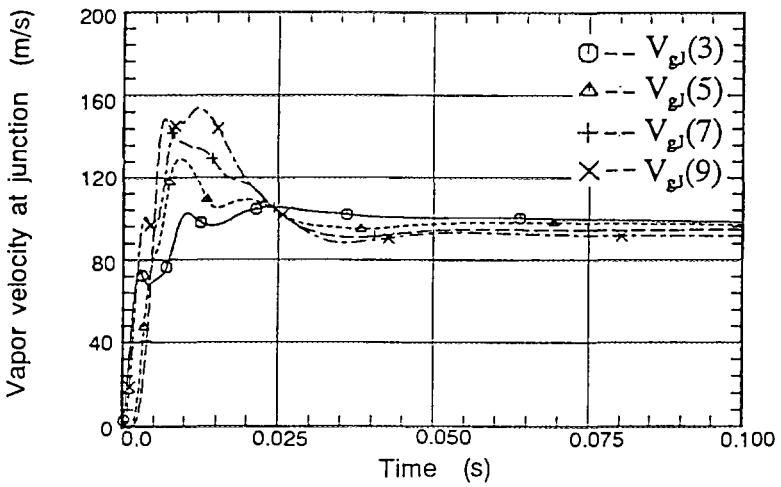

Fig.34 Vapor velocities at Junction 3,5,7,9 (case.3)

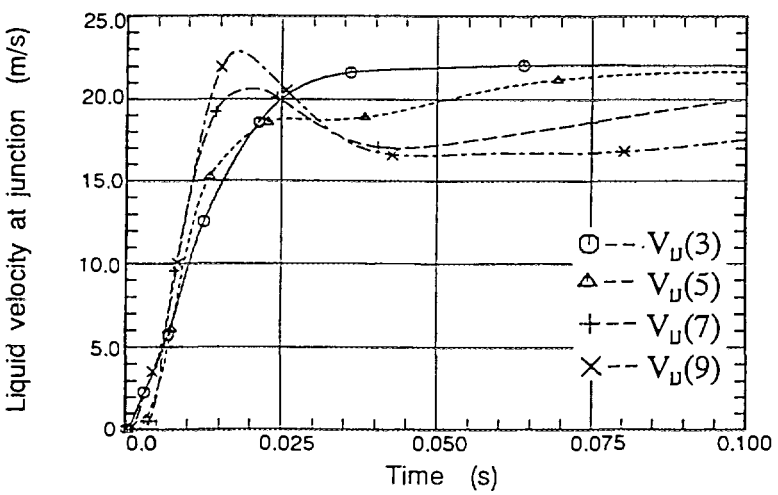

Fig.35 Liquid velocities at Junction 3,5,7,9 (case.3)

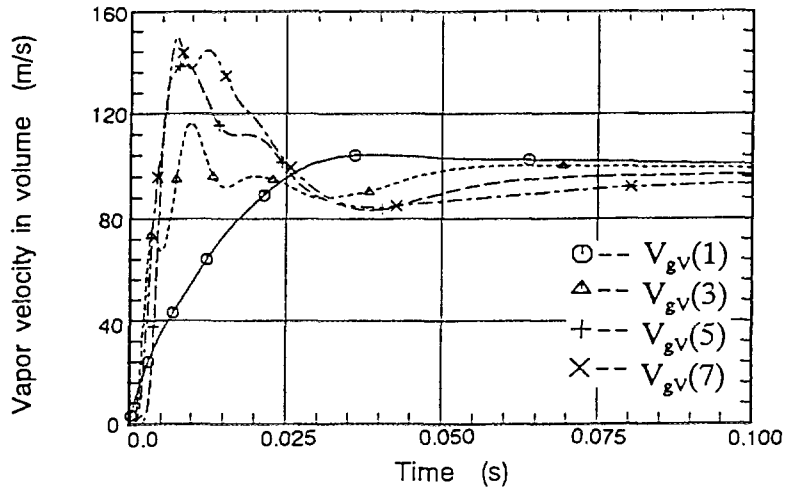

Fig.36 Vapor velocities in Volume 1,3,5,7 (case.3)

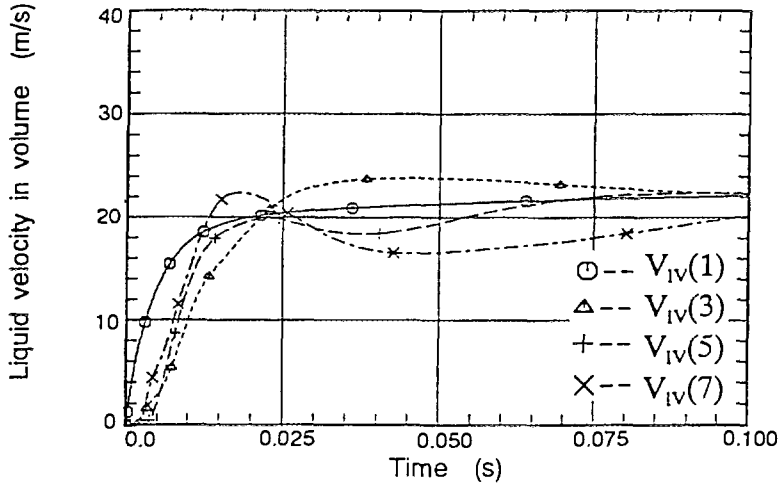

Fig.37 Liquid velocities in Volume 1,3,5,7 (case.3)

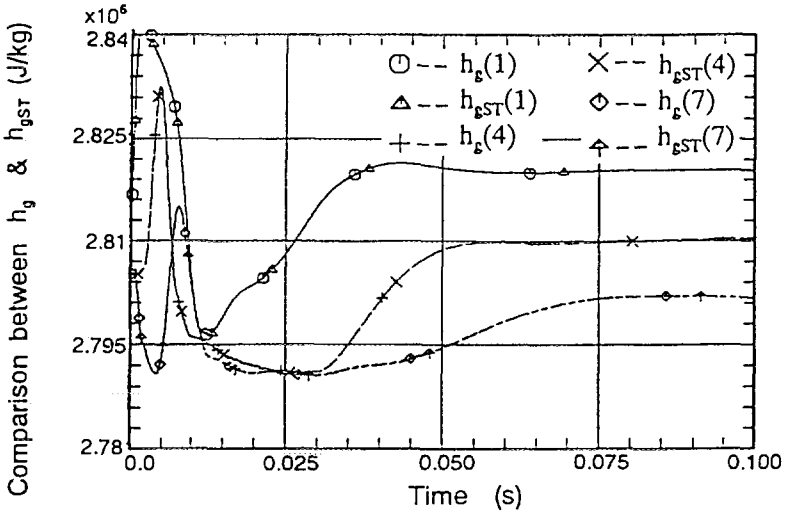

Fig.38 Comparison of specific vapor enthalpies in Volume 1,4,7 (case.3)

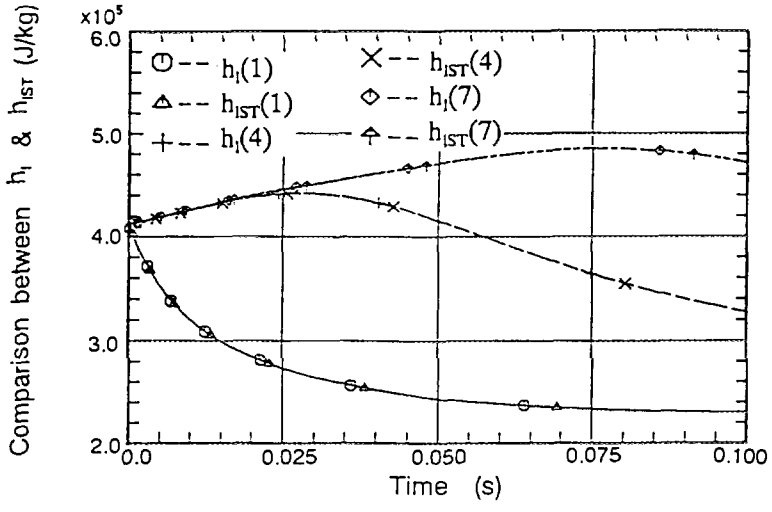

Fig.39 Comparison of specific liquid enthalpies in Volume 1,4,7 (case.3)

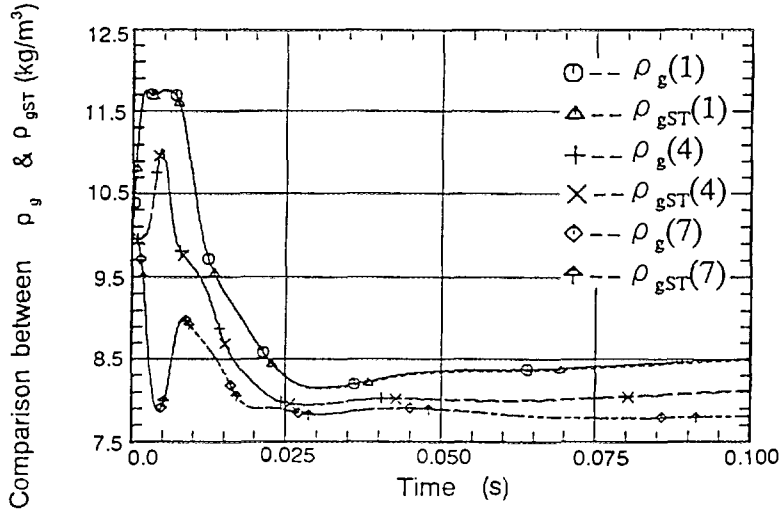

Fig.40 Comparison of vapor densities in Volume 1,4,7 (case.3)

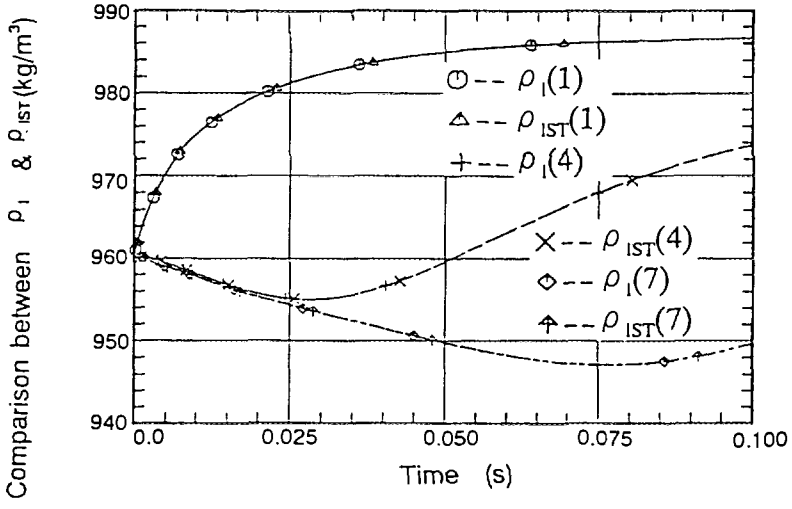

Fig.41 Comparison of liquid densities in Volume 1,4,7 (case.3)

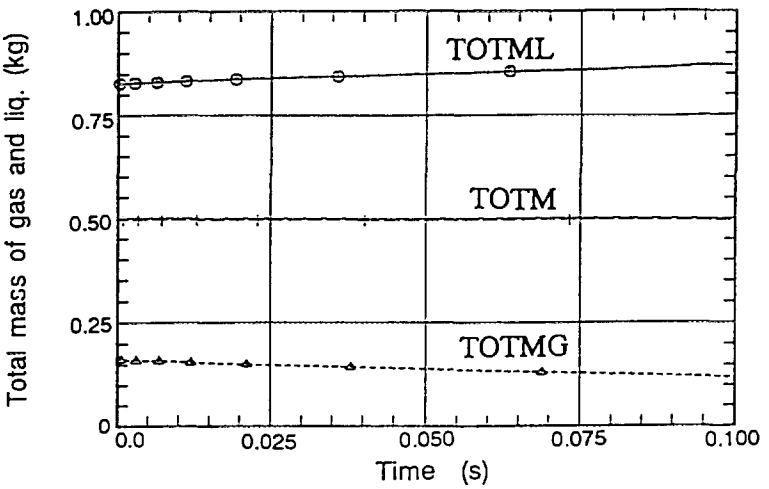

Fig.42 Total mass of vapor and liquid including discharged one. (case.3)

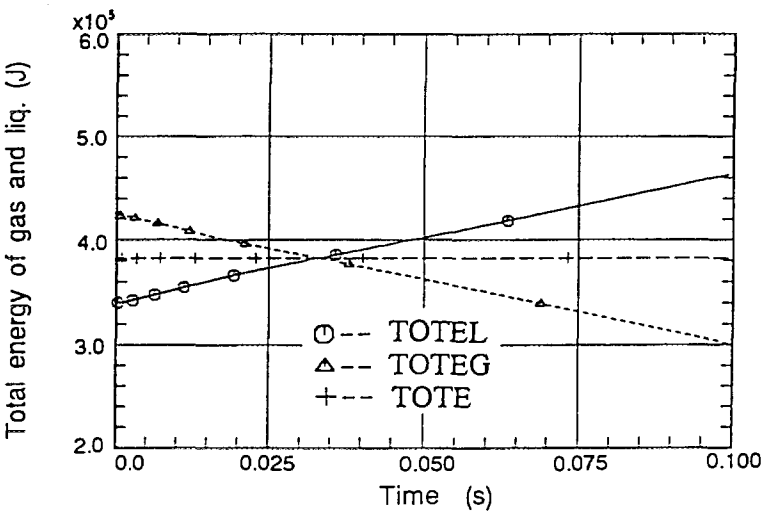

Fig.43 Total energy of vapor and liquid including discharged one. (case.3)

国際単位系 (SI) と換算表

表1　SI基本単位および補助単位

量	名称	記号
長さ	メートル	m
質量	キログラム	kg
時間	秒	s
電流	アンペア	A
熱力学温度	ケルビン	K
物質量	モル	mol
光度	カンデラ	cd
平面角	ラジアン	rad
立体角	ステラジアン	sr

表2　SIと併用される単位

名称	記号
分，時，日	min，h，d
度，分，秒	°，′，″
リットル	l，L
トン	t
電子ボルト	eV
原子質量単位	u

1 eV=1.60218×10^{-19}J

1 u=1.66054×10^{-27}kg

表3　固有の名称をもつSI組立単位

量	名称	記号	他のSI単位による表現
周波数	ヘルツ	Hz	s^{-1}
力	ニュートン	N	$m\cdot kg/s^2$
圧力，応力	パスカル	Pa	N/m^2
エネルギー，仕事，熱量	ジュール	J	N·m
工率，放射束	ワット	W	J/s
電気量，電荷	クーロン	C	A·s
電位，電圧，起電力	ボルト	V	W/A
静電容量	ファラド	F	C/V
電気抵抗	オーム	Ω	V/A
コンダクタンス	ジーメンス	S	A/V
磁束	ウェーバ	Wb	V·s
磁束密度	テスラ	T	Wb/m^2
インダクタンス	ヘンリー	H	Wb/A
セルシウス温度	セルシウス度	℃	
光束	ルーメン	lm	cd·sr
照度	ルクス	lx	lm/m^2
放射能	ベクレル	Bq	s^{-1}
吸収線量	グレイ	Gy	J/kg
線量当量	シーベルト	Sv	J/kg

表4　SIと共に暫定的に維持される単位

名称	記号
オングストローム	Å
バーン	b
バール	bar
ガル	Gal
キュリー	Ci
レントゲン	R
ラド	rad
レム	rem

1 Å=0.1 nm=10^{-10}m

1 b=100 fm^2=10^{-28} m^2

1 bar=0.1 MPa=10^5Pa

1 Gal=1 cm/s^2=10^{-2} m/s^2

1 Ci=3.7×10^{10}Bq

1 R=2.58×10^{-4}C/kg

1 rad=1 cGy=10^{-2}Gy

1 rem=1 cSv=10^{-2}Sv

表5　SI接頭語

倍数	接頭語	記号
10^{18}	エクサ	E
10^{15}	ペタ	P
10^{12}	テラ	T
10^{9}	ギガ	G
10^{6}	メガ	M
10^{3}	キロ	k
10^{2}	ヘクト	h
10^{1}	デカ	da
10^{-1}	デシ	d
10^{-2}	センチ	c
10^{-3}	ミリ	m
10^{-6}	マイクロ	μ
10^{-9}	ナノ	n
10^{-12}	ピコ	p
10^{-15}	フェムト	f
10^{-18}	アト	a

（注）

1. 表1－5は「国際単位系」第5版，国際度量衡局 1985年刊行による。ただし，1 eVおよび1 uの値はCODATAの1986年推奨値によった。
2. 表4には海里，ノット，アール，ヘクタールも含まれているが日常の単位なのでここでは省略した。
3. barは，JISでは流体の圧力を表わす場合に限り表2のカテゴリーに分類されている。
4. EC閣僚理事会指令ではbar，barnおよび「血圧の単位」mmHgを表2のカテゴリーに入れている。

換算表

力	N(=10^5dyn)	kgf	lbf
	1	0.101972	0.224809
	9.80665	1	2.20462
	4.44822	0.453592	1

粘度　1 Pa·s(N·s/m^2)=10 P(ポアズ)(g/(cm·s))

動粘度　1 m^2/s=10^4St(ストークス)(cm^2/s)

圧力	MPa(=10 bar)	kgf/cm^2	atm	mmHg(Torr)	lbf/in^2(psi)
	1	10.1972	9.86923	7.50062×10^3	145.038
	0.0980665	1	0.967841	735.559	14.2233
	0.101325	1.03323	1	760	14.6959
	1.33322×10^{-4}	1.35951×10^{-3}	1.31579×10^{-3}	1	1.93368×10^{-2}
	6.89476×10^{-3}	7.03070×10^{-2}	6.80460×10^{-2}	51.7149	1

エネルギー・仕事・熱量	J(=10^7erg)	kgf·m	kW·h	cal(計量法)	Btu	ft·lbf	eV
	1	0.101972	2.77778×10^{-7}	0.238889	9.47813×10^{-4}	0.737562	6.24150×10^{18}
	9.80665	1	2.72407×10^{-6}	2.34270	9.29487×10^{-3}	7.23301	6.12082×10^{19}
	3.6×10^6	3.67098×10^5	1	8.59999×10^5	3412.13	2.65522×10^6	2.24694×10^{25}
	4.18605	0.426858	1.16279×10^{-6}	1	3.96759×10^{-3}	3.08747	2.61272×10^{19}
	1055.06	107.586	2.93072×10^{-4}	252.042	1	778.172	6.58515×10^{21}
	1.35582	0.138255	3.76616×10^{-7}	0.323890	1.28506×10^{-3}	1	8.46233×10^{18}
	1.60218×10^{-19}	1.63377×10^{-20}	4.45050×10^{-26}	3.82743×10^{-20}	1.51857×10^{-22}	1.18171×10^{-19}	1

1 cal = 4.18605 J(計量法)
= 4.184 J (熱化学)
= 4.1855 J (15 °C)
= 4.1868 J(国際蒸気表)

仕事率　1 PS(仏馬力)
= 75 kgf·m/s
= 735.499 W

放射能	Bq	Ci
	1	2.70270×10^{-11}
	3.7×10^{10}	1

吸収線量	Gy	rad
	1	100
	0.01	1

照射線量	C/kg	R
	1	3876
	2.58×10^{-4}	1

線量当量	Sv	rem
	1	100
	0.01	1

（86年12月26日現在）

A SIMPLE AND RATIONAL NUMERICAL METHOD OF TWO-PHASE FLOW WITH VOLUME-JUNCTION MODEL,(II)